A novel approach of using electrostatic field to improve economic losses during thawing and maintaining frozen beef quality

by

Grace Elizabeth Corrette

B.S., University of Wyoming, 2021

A THESIS

submitted in partial fulfillment of the requirements for the degree

MASTER OF SCIENCE

Department of Animal Sciences and Industry
College of Agriculture

KANSAS STATE UNIVERSITY
Manhattan, Kansas

2023

Approved by:

Major Professor
Michael D. Chao

Copyright

Abstract

Freezing is a long-practiced intervention to preserve meat quality during storage. However, the formation of ice crystals during freezing can cause physical damage to cell membrane resulting in negative impacts on quality characteristics. Therefore, the objective of this study was to evaluate the impact of applying an emerging technology of electrostatic field (EF) assisted thawing on the quality attributes of beef striploin. Beef striploins from both sides of 12 USDA Choice carcasses were halved, frozen at -40 ^{o}C and thawed under 4 EF voltage treatments: 0 kV (control), 2.5 kV, 5 kV, and 10 kV. After reaching the internal temperature of -1°C, striploins were weighed and swabbed for microbial content. Available purge was collected for protein concentration and microbial analysis, and then striploins were fabricated into steaks. The steaks were assigned to either 0- or 14- days aging and retail displayed for 0- or 7- days. During retail display, steaks were evaluated for discoloration and objective color measurements. Upon completion of retail display, steaks were utilized for Warner-Bratzler shear force (WBSF), cook loss, sarcomere length, troponin-T protein degradation, lipid oxidation, antioxidant capacity, pH, and proximate analysis. It was found that EF treatments increased purge loss compared to the control (P<0.05) and did not improve thawing speed (P>0.05), with 10kV EF taking longest to thaw (P<0.05). The 2.5 kV EF tended to decrease muscle fiber spacing compared to the control (P=0.09). There was no impact on aerobic plate counts for all EF voltages on the purge as well as the swabs on the surface (P>0.05). Samples aged for 0 days under 5kV EF showed more discoloration than those from the other treatments (P<0.05), and samples aged 14 days under 2.5kV and 5kV EF showed less discoloration than those from 0 kV and 10kV (P<0.05). Samples thawed under 10kV EF showed a reduction in WBSF compared to the control (P<0.05), but there was no impact of EF on microbial content, sarcomere length,

troponin-T degradation, relative fat %, crude protein %, or moisture %, purge protein concentration, pH, lipid oxidation and antioxidant capacity for both the hydrophilic and lipophilic portion (P>0.05). Overall, our study found that there was no benefit to applying EF during thawing on yield and purge losses to provide an economic incentive. However, there are findings that indicate that the application of EF may improve tenderness and extend shelf-life of beef during retail display.

Table of Contents

List of Figures

List of Tables

Acknowledgements

When I started at Kansas State University, I did not know where my journey was going to take me. I am so beyond grateful that my journey led me to have the pleasure to work with Dr. Chao. So I would like thank Dr. Chao first and foremost. Thank you, for believing in me, guiding me, pushing me, inspiring me, and ultimately for helping me to become the best scientist, teammate, and person that I could be. The experiences and mentoring you gave me have changed who I am as a person and changed my life, and I cannot thank you enough.

I would like to thank my committee members, Dr. Morgan Zumbaugh and Dr. Scott Eilert, for investing in me. Your time and guidance has been invaluable and I have been extremely lucky to have such excellent mentors through this process. I would also like to thank the other meat science faculty, especially Sally, who all had a role in aiding me and helping me grow. I have learned so much from all of you.

Next, I would like to thank all of the graduate and undergraduate students that have been with me through all the good and bad: Haley, Erin, Hope, Vannith, and everyone else who has been with me in the office and lab through the years. I could not have done this without your support, your willingness to help, and your friendship. Thank you for the all the laughs, the stories, and as always with me, all the memes.

Linnea, words are not able to express how grateful I am that our paths crossed at the time that they did and how glad I am that I decided the second I met you that you were going to be my best friend. It's not every day you meet someone who matches your energy and soul the way you have for me. I am so lucky to have the absolute privilege of having you in my life and I cherish every moment we have together. I cannot wait to build many more memories and puzzles with you.

There have been so many people outside of K-state that have supported me on my journey that I am grateful for (Hunter and my McGees), but I would like to especially thank Danielle. I could not have asked for better person to brave the storms that life had to throw at us with. You have always supported me, made me laugh, and have been my rock. Thank you for bringing me Hazel and encouraging me to bring spiders into the house. You coming to Manhattan was the best unexpected present I could have ever received.

Finally, I would like to thank my amazing loving family: my mom, my dad, my brother Jack, and my sister Jackie. I could not have done this without your endless love and support. You have no idea how much it meant to me that you were always willing to guide me, listen to me ramble about my research, help me with my dilution calculations and statistics, and overall support me in this crazy journey. When I started, I had the mindset that I had to stand and succeed on my own. Through this process, I have learned that you can never do it alone, and I have had the greatest privilege to experience you always being there for me, my greatest support system, my biggest fans. I love you all so much.

Dedication

This work is dedicated to my amazing loving parents. I would not be where I am today without your endless love, encouragement, and support. You taught me to never give up and to strive for every dream I had. You have helped me become a person I am proud of and I cannot thank you enough for everything you have done for me.

Chapter 1 - Review of Literature

Introduction

Freezing is a long-practiced method of cold chain management used to prolong the shelf-life of meat products as it serves as an effective way to maintain the safety, nutritional value, taste, and textural characteristics of meat products (Delgado and Sun, 2001). Freezing functions to improve shelf-life by reducing available liquid water for microorganisms to utilize and slowing down the rate of chemical reactions (Calvelo, 1981). However, freezing is not perfect, as the formation of ice crystals can damage the cell membrane, which as a result can impact the yield and quality characteristics of frozen foods. The impact of freezing and thawing on frozen food items is determined by the extent of cellular dehydration as well as the formed ice crystal size and location (Li and Sun, 2002). Therefore, technologies such as high-pressure, ultrasound, magnetic and electrostatic fields assisted freezing and thawing have been developed to mitigate the negative impacts of ice crystal formation (Cai et al., 2019). This literature review will focus on understanding freezing and thawing processes and how innovative technology like electrostatic field may be able to mitigate the impacts of freezing and thawing on thawed meat characteristics.

Traditional Freezing and Thawing – Overview

Freezing of Meat

Freezing meat involves removing heat from the product to a point where the free water in the meat product is converted into bound water in the form of ice (Van der Sman and Boer, 2005). The water present in meat freezes at a lower temperature than pure water due to the presence of solutes such as sodium (Leygonie et al., 2012). Therefore, complete freezing in meat occurs at around -2°C, as opposed to water at 0°C (Lawrie and Ledward, 2014). The process of

ice crystal formation, or crystallization, occurs in two major steps: nucleation and crystal growth. As the temperature of meat product continuously drops and cools towards the center, water molecules will gradually align, resulting in the formation of an ice crystal nucleus, which the crystal structures will form off of crystal nuclei and increase in size and structure complexity throughout the freezing process (Hu et al., 2013). The formation of these nuclei holds high importance when considering the impact of freezing on a food product, as this process ultimately determines the number of ice crystals that will form, as well as the final ice crystal morphology (Kiani and Sun, 2011).

Freezing Rate

The processes and outcome of nucleation and resulting crystallization are highly influenced by temperature and freezing rate, which can influence ice crystal size, shape, and distribution throughout the product (Hu et al., 2013). When the freezing rate increases, the rate of nucleation also increases, thus resulting in more nuclei being formed. Therefore, faster freezing rates result in more numerous, but ultimately smaller ice crystals (Fennema et al., 1973). In contrast, nucleation occurs much slower at slow freezing rates, resulting in free water aggregation and form into larger ice crystals. Larger ice crystals in the extracellular space have been shown to increase mechanical damage to the membrane of the muscle fibers (Añón and Calvelo, 1980). The damage done to the muscle fibers forms holes in the membrane that allows for free water in the intracellular space to move into the extracellular space during thawing (Kiani and Sun, 2011). Thus, ice crystal morphology highly dictates the impacts of thawed meat quality as well as the amount of water that is lost as purge during thawing.

Thawing of Meat

Thawing refers to the conversion of water from a solid state to liquid state as a result of exposure to warmth. Thawing reveals the damage of the food product caused by freezing and ice crystal formation. For meat, the biggest concern associated with thawing of previously frozen meat is the increased purge loss, which it results in significant economic losses for meat processors and retailers as the weight of the product decreases with the lost moisture content (Watanabe et al., 2018) It is important to note that an extent of moisture loss is inevitable, as the process of the conversion of muscle to meat during post mortem metabolism results in overall decreased water holding capacity through a decrease in pH closer to the isoelectric point of the muscle proteins (Huff-Lonergan and Lonergan, 2005). However, it has been well established that the processes of freezing and thawing can increase the amount of purge loss (Añón and Calvelo, 1980; Ngapo et al., 1999). The severity of the loss is highly dependent on the freezing rate that dictates the final ice crystal morphology and consequential damage. For example, Añón and Calvelo (1980) found that when freezing beef, the amount of purge loss markedly increased when time to reach the final frozen temperature was beyond 19.5 minutes, demonstrating that increased purge loss is observed as an outcome of larger extracellular crystals formation.

Thawing Rate

Thawing rate can also greatly impact the extent of purge loss. When the rate in which muscle fibers can reabsorb free water is equal to rate of the ice crystals melting, the meat product will be able to retain the most water (Gonzalez-Sanguinetti et al., 1985). An increase in purge loss was observed when the rate of the ice crystals melting is faster than the rate the muscle fibers can reabsorb the liquid water, resulting in the free water being present in the extracellular space and escape the product (Leygonie et al., 2012). However, Gonzalez-Sanguinetti et al.

(1985) found that as time to reach thawed temperature was decreased, there was a subsequent decrease in purge loss when beef was thawed at lower temperatures. This relationship of faster thawing time and decreased purge loss was also observed when thawing frozen salmon at 5ºC compared to 25ºC (Haugland, 2002). This could be explained that when meat is thawed at lower temperatures, the rate of which ice crystals are converted to liquid water is at a slow enough rate for the dehydrated muscle fibers to reabsorb the water. This phenomenon requires a delicate balance of thawing environment temperatures, as well as time on the overall rate of freezing on resulting purge losses. However, to make matters more complicated, there is another phenomenon that can negatively impacts purge loss. As ice melts coupled with temperature fluctuations during thawing, water molecules can reform into ice crystals resulting in recrystallization (Vicent et al., 2019). These ice crystals are larger and irregular and can further increase in mechanical damage (Vicent et al., 2019). If thawing conditions allow for an increased level of recrystallization, there can be a subsequent increase in purge, even if the initial freezing conditions encouraged small uniform crystals to form. At warmer temperatures, the mobility of water is increased and able to form larger ice crystals (Syamaladevi et al., 2012). Therefore, the rate of recrystallization can be controlled by ensuring proper storage conditions with minimal temperature fluctuations during thawing.

Thawed Meat Quality – Sensory Characteristics

Freezing and thawing can also impact sensory characteristics of meat such as color, lipid oxidation, and tenderness (Dalvi-Isfahan et al., 2016). As mentioned earlier, the formation of ice crystals can damage the cellular and organelle membranes and release mitochondrial and lysosomal enzymes into the sarcoplasm (Hamm, 1979), and the increased release of mitochondrial and lysosomal enzymes may negatively impact color through an increased rate of

oxygen consumption in the meat product, causing additional formation of metmyoglobin which can result in the formation of brown pigments (Tsvetkov et al., 1985). Lipid oxidation is seen to occur throughout frozen storage, even at low temperatures (Soyer et al., 2010). In fact, the chemical reactions responsible for lipid oxidation can be enhanced during frozen storage as a result of the solute concentration increasing due to the water being removed in the ice crystals (Fennema et al., 1973). This effect can be explained by the process of ice crystal formation resulting in damage to the cell membranes and organelles, which can cause pro-oxidants, such as nonheme iron, to leak out and increase lipid oxidation after thawing (Benjakul and Bauer, 2001).

Another quality attribute that is notably impacted by the process of freezing is tenderness. Meat that has been frozen and thawed has shown improvements on tenderness compared to fresh meat (Lagerstedt et al., 2008). The length of storage can also impact the extent of tenderness improvement (Ablikim et al., 2016). This can be attributed to the fact that when ice crystals form, particularly larger extracellular ice crystals, they disrupt the physical structure of the myofibrils, resulting in improved tenderness (Petrović et al., 1993). However it is important to note that aging prior to freezing showed more of an effect on tenderness than the impact of freezing alone (Vieira et al., 2009).

Electrostatic Field Assisted Thawing – Overview

Function of Electrostatic Field

Electrostatic field assisted thawing is an emerging technology that is gaining popularity in developing countries due to the lower energy consumption required compared to conventional thawing methods as electrostatic field can speed up the thawing process (Cao et al., 2004; He et al., 2016). An electrostatic field involves applying an electrical current to a system at a stationary or static charge, hence the term electrostatic. Factors in which compose an electrostatic field can

be utilized include: voltage, amplitude, current, and time. In physics application, voltage is measured in volts and refers to the amount of pressure that is applied to the electrons, while amplitude applies to the distance that electrons are able to move in the system (Duit and von Rhöneck, 1997). The current refers to the direction, or flow, of the electricity being applied. The flow of a constant current does not change, staying in one set direction, while the flow of an alternating current reverses directions at a set interval (Edwards, 1971). For the purpose of this review, the voltage can be viewed as the energy supplied corresponding to the amount of pressure on the electrons, while the amplitude is the intensity of the electrical current applied over a period of time.

The principle of the electrostatic fields function relies upon the nature of the structure of water molecules. Water is a dipole molecule, meaning that there is a slight positive charge on the oxygen as well as negative charges on the hydrogen regions of the molecule, despite the overall charge of the molecule being neutral, and the electrical current can affect these charged areas of the water molecule (Jha et al., 2017). An electrostatic field may be used during freezing while the ice crystals are formed, or during thawing by affecting the ice crystals size and structure. When applied during freezing, the electrostatic field encourages the rate of nucleation for small ice crystals through a phenomenon called ‘supercooling’, and results in decreased physical damage to the product (Orlowska et al., 2009).

However, the focus of this literature review will be on how the electrostatic field impacts ice crystals size and structure when applied during thawing. When ice crystals were developed during freezing, the structure retains positively and negatively charged regions as they are formed in a concept known as charge separation (Díaz et al., 2022). These charged regions are susceptible to electrostatic field. This occurs by the positive and negative areas of the ice crystals

being attracted to the voltage electrodes, where the current is being applied, and can cause the ions to oscillate their position towards the source (Wei et al., 2008). This rapid ion oscillation of the ice crystals over time may result in the larger ice crystals breaking apart into smaller or more uniform crystals and reduce cell membrane damage (Rahbari et al., 2018).

In addition to the oscillation of ions breaking apart the ice crystals, the ion movement can cause friction energy and increase the heat transfer coefficient through a phenomenon known as "ionic wind" (Zhang and Ding, 2020). Ionic wind is an electrohydrodynamic phenomenon that occurs from electrical current passing through a system, generating an airflow. As voltage increases, the speed of the ionic wind also increases (Zhang and Ding, 2020). This increase in energy and heat can increase the conversion of ice to water, subsequently leading to an increase in the conductivity of the product, and result in improved thawing speeds. In addition to this, the increased heat transfer coefficients can inhibit recrystallization and the additional membrane damage associated with recrystallization (Ben-Yoseph and Hartel, 1998). Overall, applying an electrostatic field during thawing provides an opportunity to mitigate the repercussions associated with previously frozen meat.

Electrostatic Field Assisted Thawing – Impacts on Meat

Overview

Previous research has shown that electrostatic field assisted thawing may have some economic incentives compared to traditional cooler thawing by increasing thawed meat yield and thawing rate (He et al., 2013). In addition, electrostatic field assisted thawing allows for previously frozen meat products to more closely resemble fresh meat characteristics after thawing (Qian et al., 2019). Understanding the impact on cellular damage as well physicochemical processes from electrostatic thawing will provide insight as to what is occurring

during thawing, as well as what conditions of the electrostatic field being applied provide the most merit.

Thawing Rate & Purge Loss

The voltage, current, and amplitude of an electrostatic field thawing all play a role in altering ice crystal size and structure over thawing time, but voltage intensities can have the most impact on thawing speed of a product. He et al. (2014) observed applying voltages ranging from 4kV to 14kV on frozen pork tenderloin, and it was found that while all voltages increased thawing speed compared to traditional thawing, the higher voltages above 6kV thawed the pork tenderloin at a faster rate than those from the 4 kV treatment. This was also observed by Mousakhani-Ganjeh et al. (2015) who looked at thawing frozen tuna fish under varying voltage intensities of 4.5kV-14kV, where the higher voltages, the quicker the thawing rate. These studies explained that the increased voltage resulting increased ionic wind speeds, subsequently increasing the heat transfer coefficient.

However, there are some contradicting results in term of how electrostatic field thawing can affect purge loss. He et al. (2013) found that there was no difference in thawing loss for pork thawed between voltages 4kV to 10kV compared to the traditional thawing, and Mousakhani-Ganjeh et al. (2015) observed that all voltage treatments increased total water loss, a combined measurement of thawing and cooking loss. Contradicting to He et al. (2013) and Mousakhani-Ganjeh et al. (2015)'s findings, Qian et al. (2019) who thawed beef under a 2.5 kV electrostatic field showed a reduction in purge loss compared to samples thawed under refrigerator conditions, which the authors hypothesized that this is a result of the electrostatic field reducing disruption of the cell membranes, causing less of the cellular contents to leak out into the extracellular matrix as purge (Qian et al., 2019). On the other hand, Hsieh et al. (2010) showed

there was no difference in purge loss, cook loss, or water holding capacity compared to traditional refrigerator thawing for chicken thigh meat thawed at -3°C at 20 kV, but the electrostatic field treated samples had lower cooking loss as well as a higher water holding capacity when thawed at 4°C at 20 kV when compared to traditional refrigerator thawing. This demonstrated that thawing temperature conditions may also have an impact of the effectiveness of an electrostatic field on reducing water losses.

Microbial Impacts

Another potential function of applying electrostatic field during thawing of meat is its ability to reduce the microbial load present on the meat product. Wu et al. (2022) treated apple juice with 0.8 kV electrostatic field and found that *Escherichia coli* O157:H7 cells had irreversible membrane damage after the electrostatic field treatment. He et al. (2013) found that pork thawed under a 10 kV electrostatic field showed a 0.5-1.0 CFU/g reduction in total viable cell counts compared to traditional thawing. This was also observed by Jia et al. (2017) where rabbit meat thawed under 10-25 kV electrostatic field reduced total viable cell counts by as much as 1.6 log CFU/g as opposed to traditional thawing. Furthermore, electrostatic field has demonstrated an ability to reduce microbial content even at lower voltages. Zhang et al. (2023) found that the application of 3 kV electrostatic field can reduce total viable cell counts on large yellow croaker fish by approximately 2.0 log CFU/g compared to traditional storage over 18 days.

Sale and Hamilton (1967) hypothesized that the application of the electric field disrupted the membranes of the bacteria cells, reducing its ability to maintain the semi-permeability of the membrane to serve as a barrier from the environment, ultimately resulting in cell death. In addition, the membrane damage caused by the electrostatic field can also prevent bacterial

reproduction through division, and therefore results in a decrease in total viable cell counts (Unal et al., 2002). Overall, there is a consensus in literature that application of an electrostatic field has the ability to extend shelf-life of meat products through microbial reduction. Bacteria being present on a meat products surface has been shown to decrease shelf-life by spoilage bacteria metabolic processes resulting in lipid oxidation, off flavors and odors, and color discoloration (Papuc et al., 2017). Therefore, reducing the presence of spoilage bacteria by the application of electrostatic field presents a potential antimicrobial free method to extend shelf-life of meat.

Color Impacts

Meat that has been frozen and thawed has a decrease in color stability when compared to fresh meat products due to denaturation that takes place of the globin portion of the myoglobin molecule (Calvelo, 1981). However, consumers of meat products use visual color as an indicator of safety and predicted overall eating experience (Mancini, 2013). As a result, providing products that exhibits the color associated with a fresh meat product holds a high importance to the meat industry and retailers. There have been varying results when assessing color attributes from electrostatic field treated meat products. Hu et al. (2021) thawed pork under a 2.5 kV electrostatic field, and there was a higher proportion of metmyoglobin and decreased a* values for the electrostatic field treated pork compared to the traditionally thawed pork. However, He et al. (2013) found that there was no impact of a* and b* values on pork tenderloin thawed under 4kV-10kV electrostatic field, but L* values were increased. On the other hand, Jia et al. (2017) showed that all voltage treatments increased L*, a*, and b* values of rabbit meat compared to the still air thawed samples. Finally, research showed that beef thawed under extremely high voltage (12kV-28kV) electrostatic field can decrease L* values, but elevated a* values and improved color saturation (Tian and Ding, 2023). The impact of an electrostatic field responsible

for alteration of meat color is not yet identified, but Tian and Ding (2023) hypothesizes that the decrease in L* values is related to water loss and the ability of the water to reflect light. He et al. (2013) proposes that changes in the a* values are a result of the electrostatic field improving the binding of myoglobin with oxygen on the surface of the meat.

Tenderness

Research showed that meat that has been previously frozen showed a reduction in shear force when compared to fresh meat (Shanks et al., 2002). This can be attributed to the fact that when ice crystals form, particularly larger extracellular ice crystals, they disrupt the physical structure of the myofibrils, resulting in improved tenderness (Petrović et al., 1993). Most literature on the impact of electrostatic field regarding tenderness are in agreement the application of electrostatic field during thawing of meat can reduce shear force values. Qian et al. (2019) found that beef thawed under 2.5 kV electrostatic field had lower shear force values than beef thawed under refrigeration conditions. Furthermore, Jia et al. (2018) also found that pork tenderloin thawed under a 10kV electrostatic field expressed a higher abundance of myosin-1, which myosin-1 has been used as a biomarker for tenderness in meat products (Beldarrain et al., 2018). Although there are more research trying to decode the mystery of why electrostatic field assisted thawed meat is more tender, the true impact of the electrostatic field application on the thawed products tenderness characteristics is not yet understood.

Lipid Oxidation

Lipid oxidation is responsible to the non-microbial deterioration of quality characteristics such as flavor, odor, and color (Xia et al., 2012). Lipid oxidation naturally occurs in the progression shelf-life, but can be enhanced by temperature, light, and other storage conditions (Nieva-Echevarría et al., 2020). It has been established that application of an electrostatic field

can increase the heat transfer coefficient to increase thawing rate (Zhang and Ding, 2020). Therefore, a potential consequence of this supplied heat could involve increasing lipid oxidation, which Mousakhani-Ganjeh et al. (2016) observed that as voltage increased, lipid oxidation also increased when using electrostatic field assisted thawing of frozen tuna fish. However, this is not necessarily always the case. Zhang et al. (2023) found that beef thawed at 16 kV electrostatic field had 2.0 mg/kg less malondialdehyde content than traditionally thawed samples, but beef thawed under 28 kV electrostatic field increased lipid oxidation, having more malondialdehyde content than other voltage treatments as well as the control. What makes things even more complicated is that Jia et al. (2017) found voltage intensities ranging from 15kV to 25 kV decreased lipid oxidation values compared to the control. These studies demonstrated that there could be a threshold to the improvement on lipid oxidation and that at a high enough voltage, the heat supplied to the product may actually enhance lipid oxidation.

Conclusion

The act of freezing, while necessary for preservation, results in ice crystals that can negatively impact water holding capacity and other quality characteristics in meat. Therefore, many new technologies such as electrostatic field assisted thawing was developed to potentially mitigate the negative impacts of thawed meat yield and quality. Unfortunately, there is still conflict in literature regarding the exact nature of the electrostatic fields' impact on various meat quality attributes. Therefore, this research aims to identify the effectiveness of electrostatic field assisted thawing on yield and quality of previously frozen beef subprimals.

References

Ablikim, B., Y. Liu, A. Kerim, P. Shen, P. Abdurerim, and G. H. Zhou. 2016. Effects of breed, muscle type, and frozen storage on physico-chemical characteristics of lamb meat and its relationship with tenderness. *CyTA-J Food.* 14(1):109-116. https://doi.org/10.1080/19476337.2015.1054885.

Añón, M. C., and A. Calvelo. 1980. Freezing rate effects on the drip loss of frozen beef. *Meat Sci.* 4(1):1-14. https://doi.org/10.1016/0309-1740(80)90018-2.

Beldarrain, L. R., N. Aldai, B. Picard, E. Sentandreu, J. L. Navarro, and M. A. Sentandreu. 2018. Use of liquid isoelectric focusing (OFFGEL) on the discovery of meat tenderness biomarkers. *J. Proteomics*. 183:25-33. https://doi.org/10.1016/j.jprot.2018.05.005.

Ben-Yoseph, E., and R. Hartel. 1998. Computer simulation of ice recrystallization in ice cream during storage. *J. Food Eng.* 38(3):309-329. https://doi.org/10.1016/S0260-8774(98)00116-2.

Benjakul, S., and F. Bauer. 2001. Biochemical and physicochemical changes in catfish (Silurus glanis Linne) muscle as influenced by different freeze–thaw cycles. *Food Chem.* 72(2):207-217. https://doi.org/10.1016/S0308-8146(00)00222-3.

Cai, L., M. Cao, J. Regenstein, and A. Cao. 2019. Recent advances in food thawing technologies. *Compr. Rev. Food Sci. S.* 18(4):953-970. https://doi.org/10.1111/1541-4337.12458.

Calvelo, A. 1981. Recent studies on meat freezing. *Developments in Meat Science.* London: Elsevier Applied Science Publishers. 2:125-158.

Cao, W., Y. Nishiyama, and S. Koide. 2004. Electrohydrodynamic drying characteristics of wheat using high voltage electrostatic field. *J. Food Eng.* 62(3):209-213. https://doi.org/10.1016/S0260-8774(03)00232-2.

Chang, L., S. Lin, B. Zou, X. Zheng, S. Zhang, and Y. Tang. 2021. Effect of frying conditions on self-heating fried Spanish mackerel quality attributes and flavor characteristics. *Foods.* 10(1):98. https://doi.org/10.3390/foods10010098.

Dalvi-Isfahan, M., N. Hamdami, and A. Le-Bail. 2016. Effect of freezing under electrostatic field on the quality of lamb meat. *Innov. Food Sci. Emerg.* 37:68-73. https://doi.org/10.1016/j.ifset.2016.07.028.

Delgado, A., and D.-W. Sun. 2001. Heat and mass transfer models for predicting freezing processes–a review. *J. Food Eng.* 47(3):157-174. https://doi.org/10.1016/S0260-8774(00)00112-6.

Díaz, D., D. Garcia-Gonzalez, P. Bista, S. A. Weber, H.-J. Butt, A. Stetten, and M. Kappl. 2022. Charging of drops impacting onto superhydrophobic surfaces. *Soft Matter.* 18(8):1628-1635. https://doi.org/10.1039/D1SM01725J.

Duit, R., and C. von Rhöneck. 1997. Learning and understanding key concepts of electricity. Connecting research in physics education with teacher education 1:1-6. ISBN:0-9507510-3-0.

Edwards, D. F. A. 1971. Electronic Measurement Techniques. 1st ed. Butterworth-Heinemann, Oxford UK. ISBN:0-408-70090-4.

Fennema, O. R., W. D. Powrie, and E. H. Marth. 1973. Low-temperature preservation of foods and living matter. Marcel Dekker, New York. ISBN: 9780824711856.

Gonzalez-Sanguinetti, S., M. Anon, and A. Calvelo. 1985. Effect of thawing rate on the exudate production of frozen beef. *J. Food Sci.* 50(3):697-700. https://doi.org/10.1111/j.1365-2621.1985.tb13775.x.

Hamm, R. 1979. Delocalization of mitochondrial enzymes during freezing and thawing of skeletal muscle. *ACS Publications.* https://doi.org/10.1021/ba-1979-0180.ch009

Haugland, A. 2002. Industrial thawing of fish: to improve quality, yield and capacity. Ph.D. diss., Norwegian University of Science and Technology, Trondheim, Norway. (http://hdl.handle.net/11250/233393).

He, X., G. Jia, E. Tatsumi, and H. Liu. 2016. Effect of corona wind, current, electric field and energy consumption on the reduction of the thawing time during the high-voltage electrostatic-field (HVEF) treatment process. *Innov. Food Sci. Emerg.* 34:135-140. https://doi.org/10.1016/j.ifset.2016.01.006.

He, X., R. Liu, S. Nirasawa, D. Zheng, and H. Liu. 2013. Effect of high voltage electrostatic field treatment on thawing characteristics and post-thawing quality of frozen pork tenderloin meat. *J. Food Eng.* 115(2):245-250. http://dx.doi.org/10.1016/j.jfoodeng.2012.10.023.

He, X., R. Liu, E. Tatsumi, S. Nirasawa, and H. Liu. 2014. Factors affecting the thawing characteristics and energy consumption of frozen pork tenderloin meat using high-voltage electrostatic field. *Innov. Food Sci. Emerg.* 22:110-115. https://doi.org/10.1016/j.ifset.2013.12.019.

Hsieh, C. W., C. H. Lai, W. J. Ho, S. C. Huang, and W. C. Ko. 2010. Effect of thawing and cold storage on frozen chicken thigh meat quality by high-voltage electrostatic field. *J. Food Sci.* 75(4):193-197. http://dx.doi.org/10.1111/j.1750-3841.2010.01594.x.

Hu, F., S. Qian, F. Huang, D. Han, X. Li, and C. Zhang. 2021. Combined impacts of low voltage electrostatic field and high humidity assisted-thawing on quality of pork steaks. *LWT-Food Sci. Technol.* 150:111987. https://doi.org/10.1016/j.lwt.2021.111987.

Hu, F., D.-W. Sun, W. Gao, Z. Zhang, X. Zeng, and Z. Han. 2013. Effects of pre-existing bubbles on ice nucleation and crystallization during ultrasound-assisted freezing of water and sucrose solution. *Innov. Food Sci. Emerg.* 20:161-166. https://doi.org/10.1016/j.ifset.2013.08.002.

Huff-Lonergan, E., and S. M. Lonergan. 2005. Mechanisms of water-holding capacity of meat: The role of postmortem biochemical and structural changes. *Meat Sci.* 71(1):194-204. https://doi.org/10.1016/j.meatsci.2005.04.022.

Jha, P. K., E. Xanthakis, V. Jury, and A. Le-Bail. 2017. An overview on magnetic field and electric field interactions with ice crystallisation; application in the case of frozen food. *Crystals.* 7(10):299. https://doi.org/10.3390/cryst7100299.

Jia, G., H. Liu, S. Nirasawa, and H. Liu. 2017. Effects of high-voltage electrostatic field treatment on the thawing rate and post-thawing quality of frozen rabbit meat. *Innov. Food Sci. Emerg.* 41:348-356. http://dx.doi.org/10.1016/j.ifset.2017.04.011.

Jia, G., S. Nirasawa, X. Ji, Y. Luo, and H. Liu. 2018. Physicochemical changes in myofibrillar proteins extracted from pork tenderloin thawed by a high-voltage electrostatic field. *Food Chem.* 240:910-916. https://doi.org/10.1016/j.foodchem.2017.07.138.

Kiani, H., and D.-W. Sun. 2011. Water crystallization and its importance to freezing of foods: A review. *Trends in Food Sci. & Tech.* 22(8):407-426. https://doi.org/10.1016/j.tifs.2011.04.011.

Lagerstedt, Å., L. Enfält, L. Johansson, and K. Lundström. 2008. Effect of freezing on sensory quality, shear force and water loss in beef M. longissimus dorsi. *Meat Sci.* 80(2):457-461. https://doi.org/10.1016/j.meatsci.2008.01.009.

Lawrie, R. A., and D. Ledward. 2014. Lawrie's meat science, 7th ed. Woodhead Publishing, Cambridge, England. ISBN:13-978-1-84569-159-2.

Leygonie, C., T. J. Britz, and L. C. Hoffman. 2012. Impact of freezing and thawing on the quality of meat. *Meat Sci.* 91(2):93-98. https://doi.org/10.1016/j.meatsci.2012.01.013.

Li, B., and D.-W. Sun. 2002. Novel methods for rapid freezing and thawing of foods–a review. *J. Food Eng.* 54(3):175-182. https://doi.org/10.1016/S0260-8774(01)00209-6.

Mancini, R. 2013. Meat color. The science of meat quality. John Wiley & Sons, New York. p. 177-198. https://doi.org/10.1002/9781118530726.ch9.

Mousakhani-Ganjeh, A., N. Hamdami, and N. Soltanizadeh. 2015. Impact of high voltage electric field thawing on the quality of frozen tuna fish (Thunnus albacares). J. *Food Eng.* 156:39-44. https://doi.org/10.1016/j.jfoodeng.2015.02.004.

Mousakhani-Ganjeh, A., N. Hamdami, and N. Soltanizadeh. 2016a. Effect of high voltage electrostatic field thawing on the lipid oxidation of frozen tuna fish (Thunnus albacares). *Innov. Food Sci. Emerg.* 36:42-47. http://dx.doi.org/10.1016%2Fj.ifset.2016.05.017.

Ngapo, T., I. Babare, J. Reynolds, and R. Mawson. 1999. Freezing and thawing rate effects on drip loss from samples of pork. *Meat Sci.* 53(3):149-158. https://doi.org/10.1016/S0309-1740(99)00050-9.

Nieva-Echevarría, B., E. Goicoechea, and M. D. Guillén. 2020. Food lipid oxidation under gastrointestinal digestion conditions: A review. *Crit. Rev. Food Sci.* 60(3):461-478. https://doi.org/10.1080/10408398.2018.1538931.

Orlowska, M., M. Havet, and A. Le-Bail. 2009. Controlled ice nucleation under high voltage DC electrostatic field conditions. *Food Res. Int.* 42(7):879-884. https://doi.org/10.1016/j.foodres.2009.03.015.

Papuc, C., G. V. Goran, C. N. Predescu, V. Nicorescu, and G. Stefan. 2017. Plant polyphenols as antioxidant and antibacterial agents for shelf-life extension of meat and meat products: Classification, structures, sources, and action mechanisms. *Compr. Rev. Food Sci. F.* 16(6):1243-1268. https://doi.org/10.1111/1541-4337.12298.

Petrović, L., R. Grujić, and M. Petrović. 1993. Definition of the optimal freezing rate—2. Investigation of the physico-chemical properties of beef M. longissimus dorsi frozen at different freezing rates. *Meat Sci.* 33(3):319-331. https://doi.org/10.1016/0309-1740(93)90004-2.

Qian, S., X. Li, H. Wang, W. Mehmood, M. Zhong, C. Zhang, and C. Blecker. 2019. Effects of low voltage electrostatic field thawing on the changes in physicochemical properties of myofibrillar proteins of bovine Longissimus dorsi muscle. *J. Food Eng.* 261:140-149. https://doi.org/10.1016/j.jfoodeng.2019.06.013.

Rahbari, M., N. Hamdami, H. Mirzaei, S. M. Jafari, M. Kashaninejad, and M. Khomeiri. 2018. Effects of high voltage electric field thawing on the characteristics of chicken breast protein. *J. Food Eng.* 216:98-106. http://dx.doi.org/10.1016/j.jfoodeng.2017.08.006.

Sale, A., and W. Hamilton. 1967. Effects of high electric fields on microorganisms: I. Killing of bacteria and yeasts. *BBA Gen. Subjects.* 148(3):781-788. https://doi.org/10.1016/0304-4165(67)90052-9.

Shanks, B., D. Wulf, and R. Maddock. 2002. The effect of freezing on Warner-Bratzler shear force values of beef longissimus steaks across several postmortem aging periods. *J. Anim. Sci.* 80(8):2122-2125. https://doi.org/10.1093/ansci/80.8.2122

Soyer, A., B. Özalp, Ü. Dalmış, and V. Bilgin. 2010. Effects of freezing temperature and duration of frozen storage on lipid and protein oxidation in chicken meat. *Food Chem.* 120(4):1025-1030. https://doi.org/10.1016/j.foodchem.2009.11.042.

Syamaladevi, R. M., K. N. Manahiloh, B. Muhunthan, and S. S. Sablani. 2012. Understanding the influence of state/phase transitions on ice recrystallization in Atlantic salmon (Salmo salar) during frozen storage. *Food Biophys.* 7:57-71. https://doi.org/10.1007/s11483-011-9243-y

Tian, Y., and C. Ding. 2023. Effect of High-Voltage Electric Field on Thawing Kinetics and Quality Characteristics of Frozen Beef. Processes. 11(9):2567. https://doi.org/10.3390/pr11092567.

Tsvetkov, T., L. Tsonev, N. Meranzov, and I. Minkov. 1985. Functional changes in mitochondrial properties as a result of their membrane cryodestruction: II. Influence of freezing and thawing on ATP complex activity of intact liver mitochondria. *Cryobiology.* 22(2):111-118. https://doi.org/10.1016/0011-2240(85)90165-8.

Unal, R., A. E. Yousef, and C. P. Dunne. 2002. Spectrofluorimetric assessment of bacterial cell membrane damage by pulsed electric field. *Innov. Food Sci. Emerg.* 3(3):247-254. https://doi.org/10.1016/S1466-8564(02)00033-4.

Van der Sman, R. 2017. Model for electrical conductivity of muscle meat during Ohmic heating. *J. Food Eng.* 208:37-47. https://doi.org/10.1016/j.jfoodeng.2017.03.029.

Vicent, V., F.-T. Ndoye, P. Verboven, B. Nicolaï, and G. Alvarez. 2019. Effect of dynamic storage temperatures on the microstructure of frozen carrot imaged using X-ray micro-CT. *J. Food Eng.* 246:232-241. https://doi.org/10.1016/j.jfoodeng.2018.11.015

Vieira, C., M. Diaz, B. Martínez, and M. García-Cachán. 2009. Effect of frozen storage conditions (temperature and length of storage) on microbiological and sensory quality of rustic crossbred beef at different states of ageing. *Meat Sci.* 83(3):398-404. https://doi.org/10.1016/j.meatsci.2009.06.013.

Watanabe, G., M. Motoyama, I. Nakajima, and K. Sasaki. 2018. Relationship between water-holding capacity and intramuscular fat content in Japanese commercial pork loin. *Asian Austral J. Anim. Sci.* 31(6):914. https://doi.org/10.5713%2Fajas.17.0640.

Wei, S., X. Xiaobin, Z. Hong, and X. Chuanxiang. 2008. Effects of dipole polarization of water molecules on ice formation under an electrostatic field. *Cryobiology.* 56(1):93-99. https://doi.org/10.1016/j.cryobiol.2007.10.173.

Wu, S., X. Xu, N. Yang, Y. Jin, Z. Jin, and Z. Xie. 2022. Inactivation of Escherichia coli O157: H7 in apple juice via induced electric field (IEF) and its bactericidal mechanism. *Food Microbiol.* 102:103928. https://doi.org/10.1016/j.fm.2021.103928.

Xia, X., B. Kong, J. Liu, X. Diao, and Q. Liu. 2012. Influence of different thawing methods on physicochemical changes and protein oxidation of porcine longissimus muscle. *LWT-Food Sci. Technol.* 46(1):280-286. https://doi.org/10.1016/j.lwt.2011.09.018.

Zhang, J., L. Fei, P. Cui, N. Walayat, S. Ji, Y. Chen, F. Lyu, and Y. Ding. 2023. Effect of low voltage electrostatic field combined with partial freezing on the quality and microbial community of large yellow croaker. *Food Res. Int.* 169:112933. https://doi.org/10.1016/j.foodres.2023.112933.

Zhang, Y., and C. Ding. 2020. The study of thawing characteristics and mechanism of frozen beef in high voltage electric field. *IEEE Access*. 8:134630-134639. https://doi.org/10.1109/ACCESS.2020.3010948.

Chapter 2 - A novel approach of using an electrostatic field to reduce thawing time and improve frozen beef quality

Introduction

Freezing is a cold-chain management method that is widely practiced by the meat industry to extend the shelf-life of beef products (Kim et al., 2015). This extension of shelf-life from freezing can reduce economic losses due to spoilage as well as maintaining a steady supply of meat for the consumers when there is a disruption in the supply chain (Heinz and Hautzinger, 2007). Unfortunately, the process of freezing and thawing can increase purge loss and cause other meat quality deterioration due to damage to the muscle cell membrane caused by ice crystals formation (Leygonie et al., 2012; Watanabe et al., 2018). Therefore, frozen beef products are often viewed as inferior to fresh, never frozen beef (Grunert et al., 2004). As a result, there is motivation from the meat industry to investigate new ways to thaw beef products that may reduce the negative impacts of freezing.

One of the novel technology aiming to improve frozen food quality is known as the electrostatic field (EF) assisted thawing device, which was first developed by Ohtsuki (1991) with the goal to mitigate thawing losses and decrease thawing time. The EF technology relies upon applying a high voltage output and a low alternating current (AC) to a frozen meat product over time, which can cause the oscillation of positive and negative ions in the ice crystals (Wei et al., 2008). The ion movement can cause friction energy and increase the heat transfer coefficient, which may decrease thawing times; but more importantly, this rapid ion oscillation of the ice crystals over time may result in the larger ice crystals breaking apart into smaller, more uniform ice crystals and potentially reduce the cell membrane damage (Rahbari et al., 2018) and allow the phospholipid bilayers to repair themselves.

EF thawing has been investigated and has displayed the potential economic incentive to decrease purge loss and increase thawing rates. It was observed by Qian et al. (2019) that applying a voltage at 2.5 kV to frozen beef striploins showed the ability to shorten thawing time by 42% and reduce purge loss by approximately 20%. This finding was also observed in Jia et al. (2017) who applied EF at 20 kV to frozen rabbit meat and showed that the thawing time was shortened by 60% and purge loss decreased by 30%. The EF assisted thawing has also demonstrated the ability to improve quality characteristics such as reducing lipid oxidation in rabbit meat (Jia et al., 2017) and decreasing microbial loads in pork tenderloins (He et al., 2013). However, none of these studies were conducted under standard industry operating environment, and the effects of EF on beef has not yet been evaluated in the U.S. Therefore, the main objective of this study was to characterize the effects of EF assisted thawing on beef quality attributes during subsequent aging and retail display.

Materials & Methods

Sample Collection and Preparation

The EF thawing system consists of a high voltage power supply equipped with a voltage controller (NDT-10KV, New Defrost Technology Inc., Taipei, Taiwan), a thawing cart consists of stainless-steel meat trays placed on a stainless-steel meat cart with rubber insulations placed on the 4 wheels of the meat cart, and a power cable with one end attached to the high voltage power supply and the other end with an alligator clip clipped on the meat cart (figure 1). The voltage applied to the system was verified using a multimeter (177, Fluke corp., Everett, WA) connected to a high voltage probe (80K-40, Fluke corp.).

Twelve USDA Choice beef carcasses were selected from a commercial processing facility in Nebraska. Striploins (*Longissimus lumborum*) from both sides of each carcass were

collected at 2 days post-mortem, vacuum packaged and transported to Kansas State University meat lab. The next day (3 days postmortem), the purge was collected aseptically from each vacuum package, and an area at approximately ~10 cm x 10 cm on the ventral side of the striploin was swabbed using a 3M™ Sponge Stick with 10 mL neutralizing buffer (3M™ Microbiology, St. Paul, MN). Following the swabbing, each striploin was portioned into 2 equal parts to result in 4 equal portions of striploin from each carcass (n=48). A Q series 4.5- inch penetration probe (THS-113-615, ThermoWorks Inc., American Fork, UT) was inserted into the geometric center of each portion, and each portion was vacuum packaged and frozen at -40°C for at least 14 days before being randomly assigned to one of the 4 EF thawing treatments: 0 kV, 2.5 kV, 5 kV or 10 kV. Four thawing periods were performed in the carcass cooler (2 ± 2°C), so each voltage treatment was repeated 4 times. Internal temperatures of all portions were recorded throughout the thawing process using a temperature logger (THS-291-401, ThermoWorks, Inc.). The thawing process was considered complete when the core temperature of all striploin portions reached at least -1°C (figure 2).

After thawing, striploin portions were swabbed on the ventral side at another ~10 cm x 10 cm area that were not previously swabbed (3M™ Sponge Stick with 10 mL neutralizing buffer, 3M™ Microbiology) and weighed. Purge was also collected aseptically for microbial and protein concentration analysis. Each striploin portion was fabricated into four 2.54 cm steaks and five 1.27 cm steaks. One 1.27 cm steak was immediately utilized for histological analysis. The 2.54 cm steaks and the remaining four 1.27 cm steaks were vacuum packaged and assigned to either 0 day or 14 days of additional aging. After completion of the designated aging periods, steaks were overwrapped with polyvinyl chloride (23,250 cc/m^2/24 h at 23°C and 0% RH; Sysco, Houston, TX) in Styrofoam trays (17S; Genpak, Charlotte, NC) lined with a tray absorbent pad (Dri-Loc

AC25; Novipax, Oak Brook, IL) and placed in a coffin style retail display case (model DMF8; Tyler Refrigeration Corp., Niles, MI) under fluorescent lighting (32 W Del-Warm White 3,000 K; Phillips Lighting Company, Somerset NJ) averaging a 2,143 ± 113 lx emission case-wide. All steaks were designated for 0- or 7-days retail display periods. The discoloration of each steak was evaluated daily by 6 trained panelists consisted of meat science faculty and graduate students. Panelists were trained prior to panels to evaluate and distinguish the forms of myoglobin, with discoloration being defined as the deoxy- and oxy- myoglobin pigment transitioned to metmyoglobin. Discoloration was scored by each panelist as percentages of the steak displaying discoloration on a scale of 0 being no discoloration was present and with 100 being that the steak was completely discolored. Samples were rotated within the display case every 24 hours to ensure equal distribution of light upon the packages.

In addition to the discoloration evaluation, objective color measurements were also collected according to AMSA Meat Color Measurement Guidelines as described in King et al. (2023). Readings for L*, a*, and b* were collected 6 times on each steak using a Hunter Lab Miniscan EZ spectrophotometer (Illuminant D65, 2.54-cm-diameter aperture, 10° observer; Hunter Associates Laboratory, Reston, VA) during each day of retail display (0-7 days). The spectrophotometer was calibrated prior to use each day using a standardized white and black tile. Steaks were randomly rotated to various locations in the case every 24 hours to ensure balanced intensity for light and temperature. The average temperature of the cases was 3°C, with two defrost cycles occurring at midnight and noon each day for 30 minutes. After completion of the designated aging and display periods, the 2.54 cm steaks designated for Warner-Bratzler Shear Force (WBSF) were vacuum-packaged and stored at -20°C until further analysis. The 1.27 cm steaks designated for lab analysis were frozen in liquid nitrogen, pulverized with commercial

blenders (model 51BL32, Waring Commercial, Torring, CT) and stored at -80°C until further analysis.

Microbial Analysis

Swabs and purge were collected from striploins portion both before thawing to establish a baseline microbial concentration and after thawing to assess effect of EF on microbial reduction. Neutralizing buffer was squeezed out of the sponges from the swabs and was serially diluted to 1, 1/10, and 1/100 in a neutral phosphate buffered saline using aseptic technique. The collected purge was also serial diluted following the same procedure. Following serial dilutions, 1 mL of each dilution was plated in duplicate on 3M™ Aerobic Plate Count (APC) petrifilm™ plates (3M™ Microbiology). The APC count plates were incubated at 37°C ± 2°C for 48 hours ± 2 hours. Per the 3M™ Petrifilm™ Interpretation Guide for Aerobic Count Plates, all red colonies grown were counted and recorded.

Histological Analysis for Muscle Fiber Spacing

The one 1.27 cm steak designated for histological analysis was immediately cored after fabrication. Three 1 cm x 1 cm x 1 cm muscle cores were collected from each steak parallel to the muscle fiber direction. Cores were suspended in Optimal Cutting Temperature medium (OCT; Thermo Fisher, Hampton, NH) in 22 mm x 22 mm x 20 mm Epredia™ plastic embedding molds (Thermo Fisher) and immediately frozen in liquid nitrogen cooled isopentane. Frozen cores in embedding molds were stored at -80°C until further analysis.

Frozen cores were cut perpendicular to the muscle fiber direction using a microtome cryostat (Microm HM 550; Thermo Fisher) to a thickness of 20 μm at -20 °C and adhered onto a positively charged microscope slide (Globe Scientific, Mahwah, NJ). Following slicing, slides were allowed to dry and come to room temperature for 15 minutes before being stained in 1%

hematoxylin for 5 minutes, rinsed in slow running deionized water (DI) for 5 minutes, submerged for 2 seconds in 50% eosin, submerged in 50% ethanol for 10 seconds, 70% ethanol for 10 seconds, 95% ethanol for 30 seconds, and a final fixative step of 100% ethanol for 30 seconds. Finally, slides were completely submerged in xylene for 1 second for 7 times and sealed with Epredia^{TM} Shandon-Mount (Thermo Fisher) with a coverslip placed over top and allowed to dry for 30 minutes before imaging. Slides were imaged at a 20x objective lens on a bright-field Nikon NIS-Elements Ti2 confocal microscope (Nikon Instruments, Tokyo, Japan), and images were captured using a Nikon DS-QiMc digital camera (Nikon Instruments). Imaging software ImageJ version 1.53 (U.S. National Institutes of Health, Bethesda, MD) was used to measure the distance between the sarcolemma of one muscle cell to the adjacent one in μm. Thirty measurements were collected from each core, for a total of 90 measurements for each sample. The average of the 90 measurements was reported as the muscle fiber spacing for each sample.

Warner-Bratzler Shear Force

The steaks were prepared following the AMSA Research Guidelines for cookery and evaluation (AMSA, 2016). Steaks were thawed at 2 ± 2°C for 24 hours prior to cooking, and steaks were weighed prior to cooking. Steaks were grilled on a Cuisine Art Griddle Deluxe Clamshell (Cuisine Art, Stamford, CT) to an internal temperature of 71°C measured by a thermometer with a metal needle inserted into the geometric center of each steak (Thermapen MK4; Thermoworks, American Fork, UT). Temperatures were monitored, and peak temperature and cooked weight of each steak were recorded. Cooked steaks were allowed to be cooled at 2°±2°C for 24 hours. Six 1.27 cm diameter cylinder samples from each cooled steak were taken parallel to the muscle fiber direction and sheared perpendicular to the muscle fiber orientation using a V-shaped WBSF blade attachment (G-R Elec. Mfg., Manhattan, KS) coupled to an

Instron Universal Testing System (Model 5569; Instron Corporation, Norwood, MA) set at a speed of 250 mm/minute. The mean shear force (kg) values of the six cores were calculated for each steak.

Purge Sarcoplasmic Protein Isolation

One mL of purge was diluted to a 1:100 ratio in 0.1M Tris-HCl, 1.25 mM EDTA, 2% SDS buffer. Protein concentration (mg/mL) was determined utilizing a Pierce BCA Protein Assay Kit (Thermo Fisher) following manufacturers guidelines.

Troponin-T Degradation

Approximately 0.2 grams of pulverized samples were weighed into tubes containing prefilled 3 mm zirconium beads and 1 mL of ice-cold ultrapure H_2O. Samples were homogenized for 30 seconds using a bead homogenizer (Bead Blaster 24; Benchmark Scientific, Sayreville, NJ) and transferred to a 1.5 mL microcentrifuge tube. Samples were centrifuged at 4,000 × g for 5 minutes. The supernatant was decanted, and the pellet was resuspended in 1 mL of ice-cold ultrapure H_2O and re-centrifuged. This process was repeated 2 more times to remove as much sarcoplasmic proteins as possible. The remaining pellet was resuspended in 1 mL of extraction buffer consisting of 0.1M Tris-HCl, 1.25 mM EDTA and 2% SDS buffer. Samples were vortexed thoroughly, centrifuged at 4,000 x g for 5 minutes, and the supernatant was removed as final protein stock. Protein stock concentration was determined utilizing a Pierce BCA Protein Assay Kit (Thermo Fisher) following manufacturers guidelines. Protein stock concentration of each sample was adjusted to 2,000 μg/mL before further analysis.

Troponin-T degradation was analyzed using methods described in Hammond et al. (2022). Myofibrillar proteins from each sample was combined with Laemmli SDS sample buffer with reducing agent (J63615; Alfa Aesar, Haverhill, MA) at 1:1 ratio and was heated on a heat

block for 95°C for five minutes. For each gel, 5 μL of Fisher Bioreagents protein ladder (Thermo Fisher) was loaded into the first lane of the gel for reference and band identification. Following the protein ladder, 5 μg of myofibrillar protein were loaded into the remain wells of a 10% Tris-Glycine gel (XP00100PK2; Invitrogen, Carlsbad, CA) and ran using a Mini Gel Tank (Invitrogen) filled with ice-cold tris-glycine SDS running buffer at a constant voltage of 180 V for 50 minutes. Following gel electrophoresis, the proteins were transferred to iBlot™ 2 PVDF Regular Stacks (Invitrogen, Life Technologies Ltd.) using iBlot™ 2 gel transfer device with settings of 20 V for 1 minute, 23 V for four minutes, and 25 V for two minutes. All blots were blocked for 60 minutes with OneBlock™ Western-FL Blocking Buffer (Genesee Scientific, San Diego, CA). After blocking, 10 mL of the anti-Troponin-T mouse monoclonal primary antibody (Millipore Sigma, Burlington, MA) at 1:2,000 dilution in blocking buffer was added to membranes and incubated at room temperature for 1 hour. Following incubation, 3 washes with 1X TBS-Tween at 5 minutes each were conducted on each membrane. Following the wash, 15 mL of secondary antibody (anti-mouse IgG Alexa Fluor™ Plus 488; A32723; Invitrogen) was added at 1:5,000 dilution in the blocking buffer and incubated for 1 hour at room temperature. Following incubation, 3 washes with 1X TBS-Tween and 1 final wash of 1X TBS at 5 minutes each were conducted on each membrane. The membrane was imaged using the 488 nm wavelength in the iBright Imaging System (FL1500, Thermo Fisher) and analyzed using iBright Analysis Software (Thermo Fisher). Troponin-T degradation was determined by dividing the band intensity of the identified degraded bands by the intensity of all identified troponin-T bands within the same lane and was reported as a relative percentage.

Sarcomere Length

Sarcomere length was assessed using the methods described in Hammond et al. (2022). A few speckles of pulverized sample were sprinkled onto a charged slide (Globe Scientific) and allowed to dry for 10 minutes. A hydrophobic pen (Daido Sangyo Co., Tokyo, Japan) was used to make a border around the spread sample. Two hundred and fifty μL of monoclonal anti-α-actinin anti- mouse primary antibody (Sigma-Aldrich, St. Louis, MO) at 1:5,000 dilution in 10% horse serum/0.2% Triton-X was added to each slide and incubated overnight in a humidified box. The following day, the primary antibody was removed, and slides were rinsed 3 times with a 1X PBS solution for 5 minutes per rinse. Following rinsing, 250 μL of goat anti-mouse IgG Alexa Fluor™ Plus 488 (A32723) secondary antibody at a 1:1,000 dilution in 10% horse serum/0.2% Triton-X was added and allowed to incubate for 30 minutes in a humidified box. Slides were protected from light at all steps following secondary antibody incubation. After incubation, the secondary antibody was removed, and slides were rinsed 3 times with a 1X PBS solution for 5 minutes per rinse. After rinsing, 5-6 drops of 9:1 glycerol/PBS solution were added to the slide, a coverslip was placed on top of the slide and lightly pressed down. The coverslip was sealed with clear nail polish and allowed to dry. Slides were imaged using a 100x oil-emersion objective lens on the enhanced green fluorescent protein wavelength filter and captured using a Nikon DS-QiMc fluorescent microscopy camera (Nikon Instruments) on a Nikon NIS-Elements Ti2 confocal microscope (Nikon Instruments). A total of 3 images were imaged for each sample. ImageJ (version 1.53, U. S. National Institutes of Health) was used to measure the distance of 30 sarcomeres per sample, and the 30 measurements were averaged for each sample.

Lipid Oxidation

The extent of lipid oxidation during simulated retail display was assessed using the thiobarbituric acid reactive substances (TBARS) assay as described in Dahmer et al. (2022). For analysis, approximately 0.2 grams of the pulverized samples were weighed and recorded in prefilled bead tubes with exact weights recorded, and 1 mL of trichloroacetic acid/thiobarbituric acid (20% w/v TCA: 15% w/v TBA) and 50 μL of 3% butylated hydroxytoluene (BHT) in ethanol was added. Samples were homogenized for 45 seconds using a bead homogenizer (Bead Blaster 24; Benchmark Scientific, Sayreville, NJ) and centrifuged at 2,000 ×g for 5 minutes. Supernatant was transferred into a 12 x 75 mm glass tube. The samples were incubated at 70°C in a water bath for 30 minutes followed by an ice cold-water bath for 5 minutes. Two hundred μL of each sample were pipetted in duplicate in a 96-well microplate. A standard curve containing 0 – 25 μM of malondialdehyde (MDA) was also plated to be used for the calculation of sample MDA concentration. Plates were then read in a spectrophotometer at a wavelength of 532 nm (Eon; BioTek Instruments Inc., Winooski, VT) to determine MDA concentration. The sample MDA concentration was recorded as mg of MDA/kg of meat.

pH Analysis

The pH analysis was conducted by weighing out five grams of pulverized muscle sample into 100 mL glass beakers. Fifty mL of ultrapure H_2O was added to each sample and homogenized for 20 seconds at 10,000 rpm using a bench top homogenizer with a medium probe (Homogenizer 850, Thermo Fisher). An InLab Science Pro-ISM probe connected to a Seven Compact pH meter (Meter Toledo; Columbus, OH) was calibrated using a pH 4.0 and 7.0 standard solution prior to pH measurement. The ultimate pH of each sample was measured by placing the probe into sample homogenate under constant stirring using a magnetic stirrer.

Proximate Analysis

Moisture analysis was determined by methods outlined in a modified 950.46 AOAC oven-drying method (AOAC International, 2000a). Aluminum pans were pre-labeled and dried at 110°C for 30 minutes in a forced air oven (Isotemp, Thermo Fisher, Pittsburg, PA). Following drying, aluminum pans were weighed. Five grams of pulverized sample were then weighed, with exact weights recorded, into the aluminum pans and dried in the forced air oven for 24 hours. Samples were cooled in a desiccator for at least 30 minutes, and the final weights were recorded. Moisture percentage was calculated using the starting sample weight subtracting the final dried weight, divided by the starting sample weight, and multiplied by 100.

Crude protein was analyzed according to a modified AOAC method 992.15 (AOAC International, 2000b). 0.5 grams of pulverized sample were loaded into ceramic crucibles with exact weights recorded. Ceramic crucibles were loaded into a TruMac N (LECO Corporation, St. Joseph, MO) following calibration with ethylenediaminetetraacetic acid standards. Percent nitrogen was calculated by multiplying percent nitrogen by the nitrogen factor 6.25.

Lipid content was quantified using the method described by Folch et al. (1957) with modifications. Glass tubes were pre-labeled and dried in a forced air oven (Isotemp, Thermo Fisher) set at 100°C for 30 minutes prior to sample being added. The weight of the pre-labeled and pre-dried tubes was recorded. Half a gram of pulverized sample was weighed into a fifteen mL polypropylene conical tube with exact weights recorded. Following weighing, 1.5 mL of ultrapure H_2O, 4 mL of chloroform, and 4 mL of methanol was added to the sample. Samples were shaken for 10 minutes using a Wrist Action Shaker (Model; 75 Burrel Corporation, Pittsburg, PA). Following the shaking, 2 mL of 0.74% KCl solution was added and thoroughly vortexed, then samples were centrifuged at 1,000 x g for 5 minutes. One mL of chloroform was

extracted from the bottom layer with care to not disturb the meat and top layer and transferred into the pre-dried 16x100 mm glass tubes. Chloroform was evaporated using a nitrogen evaporator (REACTI-VAP III #TS-18826, Thermo Fisher). Test tubes were transferred back into the oven set to 100°C for 30 minutes to remove any excess moisture. Percent fat was calculated by dividing the calculated lipid weight (difference of final weight and glass tube) over grams of meat x 100.

Oxygen Radical Absorbance Capacity (ORAC)

The ORAC procedure was performed according to methods described by Chun et al. (2023). For the lipophilic portion, 1 mL of hexane was added to 0.1 grams of pulverized sample in prefilled bead tubes. Samples were homogenized for 45 seconds in the bead homogenizer and shaken for one hour at room temperature. After shaking, samples were centrifuged at 3,000 x g for 10 min, and the hexane layer was collected and evaporated under nitrogen. Seven hundred fifty μL of 7% randomly methylated, -cyclodextrin (RMCD) in 50:50; acetone:water was added to redissolve the lipophilic portion. For hydrophilic portion, 1 mL of 80% water : 20% ethanol solution was added to the same tube and homogenized for an additional 45 seconds in the bead homogenizer. Samples were centrifuged at 12,000 x g for 10 minutes. Seven hundred and fifty μL of supernatant was collected for analysis. Both lipophilic and hydrophilic portions were stored at -80°C until further analysis.

Prior to sample and standard addition to the plate, 150 μL of working solution consisting 4 uM of sodium fluorescein in 75 mM phosphate buffer was added to all wells of a black 96-well plate (3631; Corning, Corning, NY). Hydrophilic portions were further diluted 1:20 with 80% water:20% ethanol solution, and the lipophilic portions were not diluted prior to being added to the plate. Twenty-five μL of sample was added in triplicates, and the plates were incubated at

37°C for 30 minutes. After incubation, 25 µL of 2,2'-Azobis (2-amidinopropane) dihydrochloride (AAPH) solution was added to each well to initiate the reaction. A multi-mode plate microplate reader (Synergy HTX; BioTek Instruments Inc.) was used with fluorescence filters for an excitation wavelength of 485 nm and an emission wavelength of 528 nm. Fluorescence of each well was measured from the bottom every 60 seconds for 120 minutes for a total of 120 measurements. The ORAC values were measured as the net area under the curve (AUC). The net AUC is calculated by subtracting the AUC of the samples from the AUC of the blank. A standard curve was obtained by plotting Trolox concentrations (0-100µM) against their average net AUC for the hydrophilic and lipophilic portions. The final unit was calculated as µmol of Trolox equivalent per gram of meat.

Statistical Analysis

Data was analyzed using the PROC GLIMMIX procedure of SAS (version 9.4, SAS Institute, Cary, NC). Thawing time, purge loss, purge protein concentration, proximate analysis, pH analysis, sarcomere length, muscle fiber spacing were analyzed as a randomized complete block design, with each thawing period serving as the block. Cooking loss, WBSF, troponin-T degradation, lipid oxidation and ORAC were analyzed as a split-split plot where the whole plot is the EF treatments and the sub-plot is the post thawing aging period, and the sub-sub plot is the retail display days. Finally, subjective and objective meat color data were analyzed as a split-split-plot repeated-measures design with EF treatments as the whole plot and post-thawing aging period as the subplot and retail display day as the repeated-measures. The experimental unit was each EF-assisted thawing system (meat cart). The Toeplitz covariance structure was selected because it had the smallest value for Akaike's information criterion. Multiple comparisons were obtained through Tukey method, and mean separation was conducted using least-squares mean

procedures. Differences among means were detected at $P<0.05$ level using the least significant difference.

Results & Discussion

Thawing time, purge loss, and cook loss

There were no differences among the treatments in thawing time from -35°C until -5°C ($P>0.05$; figure 3). However, there was a treatment effect in thawing time from -1°C from -5°C, where the 10 kV treatment samples took longer to reach -1°C than any of the other treatments ($P<0.05$). There was also a treatment effect on purge loss ($P<0.05$). There was an increase in purge loss for the 5 and 10 kV EF treatment samples compared to the 0 kV sample, while the purge loss for 2.5 kV treatment was not different from the any other EF treatments nor the control ($P<0.05$; table 1). For cooking loss measurement, there was no three-way interaction among treatment x aging x display nor two-way interaction between treatment x aging ($P>0.10$). However, there was a tendency for treatment x display interaction for cook loss ($P=0.08$). Overall, all EF samples that were displayed for 7 days had less moisture loss during the cooking process than those from samples aged for 0 days, except for those from the 10 kV EF treated samples (figure 4; $P=0.08$).

Mousakhani-Ganjeh et al. (2016b) thawed frozen tuna fish with EF voltage ranging from 0 kV-14kV, where they found increased voltages were directly proportional to increased thawing speeds. This finding was further confirmed by Jia et al. (2017), who applied EF voltages ranging from 0 kV-25 kV to frozen rabbit meat and found that the thawing rate increased up to 60% with increased voltage. This noted improvement in thawing time found in other studies arises from the principle that the ionic movement under the influence of EF can increase friction energy and heat transfer coefficient in meat (Rahbari et al., 2018). While these studies all demonstrated that as

voltage increases thawing times should decrease, our results contrasted these findings, which we showed that the frozen striploins from the 10 kV treatment actually had the longest thawing time. This is the first known study that utilized frozen striploin halves (~2.7 kg) under EF thawing, while the other previously mentioned studies looked at small piece of individual muscles. It is possible that the difference of sample size could explain the lack of improvement on thawing speed from EF application in our study.

Qian et al. (2019) found that beef striploin thawed under the application of 2.5 kV EF had less purge loss compared to those thawed at room temperature. Furthermore, Jia et al. (2017) found that applying 20 - 25 kV to frozen rabbit meat during thawing can improve water-hold capacity compared to those from lower voltage treatment (15 kV) and 0 kV treatment. In our study, both 5 and 10 kV EF samples had increased purge loss compared to the control. Since the EF device used in this study is on AC, and the higher the intensity of EF voltage, the stronger the force for the ions to oscillate in the direction of the charges of the current (Fagan et al., 2005; Lu et al., 2022). We hypothesize that the 10 kV treatment's intensity amplified ion movement to a degree that resulted in additional muscle structure damage or protein denaturation from the heat, thus leading to more free water being lost as purge. Costa et al. (1999) observed that the loss of free water can negatively impact the heat transfer coefficient in potatoes. Perhaps, the reason why all samples thawed equally until -5°C was because all water was still in ice form at that point, and the ice was starting to melt and turned into liquid water from -5°C to -1°C, which the increased purge loss in the 10 kV samples negatively affected the thawing speed due to a reduction in heat transfer coefficient.

Mousakhani-Ganjeh et al. (2015) thawed frozen tuna fish with EF voltage ranging from 0 kV-14kV and found that all EF treatments increased cooking loss. This was also observed by

Rahbari et al. (2018), who thawed frozen chicken breast under EF voltages ranging from 0-18kV and found that the application of EF regardless of voltage increased cooking loss. However, Hsieh et al. (2010) observed no thawing loss nor cook loss difference while thawing frozen chicken breast at 20 kV compared to conventional thawing at -3ºC. In our study, the 10 kV samples aged for 7 days had greater cooking loss compared to those from the control and the 2.5 kV treatment, which again demonstrated that application of high voltage EF can reduce water holding capacity. Finally, when meat is retail displayed, there is an extent of moisture loss through purge loss and dehydration, so it was expected to see a lower moisture content in meat products after display (Kropf and Zerby, 2002). However, the 10 kV treated samples had similar cooking loss regardless of retail display, which could be explained by the finding that the 10 kV treated samples also had increased purge loss during the thawing process compared to the control, and thus had less free water to be lost during the cooking process.

Microbial Analysis

There was no treatment effect for the swab nor purge APC data ($P>0.05$; table 1). He et al. (2013) observed that pork tenderloin decreased in total microbial counts when thawed under 4-10 kV EF treatments, and Zhang et al. (2023) found that the application of 3 kV EF reduced total viable cell count in large yellow croaker fish compared to those received no EF treatment. Wu et al. (2022) further confirmed the effect by investigating *Escherichia coli* O157:H7 survival rate in apple juice that was treated with an 0.8 kV EF, which they noted the EF caused irreversible cell membrane ruptures in the cells. Both Sale and Hamilton (1967) and Unal et al. (2002) further confirmed that the application of EF can disrupted the semi-permeability of the cell membrane and its ability to protect the bacteria cell from the environment, ultimately resulting in cell death and reduction of total viable cell counts in food applications. However, our

finding are not consistent with the previously mentioned studies in showing consistent reduction in the total APC. Hsieh et al. (2010) also found no increase in total viable counts for chicken meat thawed at -3ºC, and Li et al. (2017) found that common carp thawed under 6kV EF had a final microbial load similar to the control. The cooler temperatures in our study ranged from 0-2ºC and the temperature of the product was around -1ºC. These lower temperatures could have been the contributing factor that controlled the growth of bacteria and showed no differences in APC in our study, regardless of the voltage applied for both the external surface as well as the purge.

Proximate Analysis, Purge Protein Concentration, and pH measurements

There was no treatment effect on percentages of moisture, protein or fat, protein concentration in the purge nor pH of the samples ($P>0.05$; table 1). It was expected that EF will not alternate the protein and fat content. However, it was to our surprise that no EF effect was found for moisture content as the 5 and 10 kV EF samples had statistically greater purge losses compared to those from the other treatments. However, it is important to note that the difference between these treatments was less than 1%, and that small difference can explain the lack of impact of EF treatments on total moisture content.

Qian et al. (2019) noted less protein present in the purge from beef striploin thawed under 2.5kV EF compared to traditional thawing. The same authors hypothesized that as EF can decrease damage to the muscle cell membrane, less of the sarcoplasmic cellular contents leaked out of the cells into the extracellular space. Additionally, Traore et al. (2012) also found that exudate content can indicate the degree of protein denaturation and oxidation. However, our finding likely means that the EF treatments from our study did not reduce any damage from the ice crystal formation nor reduce any protein denaturation, thus protein concentration in the purge

was not reduced from the EF applications. Finally, both Jia et al. (2017) and He et al. (2013) evaluated the effect of EF on pH in rabbit meat and pork loin thawed under EF, respectively, and they both found that EF treatments had no impact on pH of thawed meat products, which agreed with our findings.

Sarcomere Length, Muscle Fiber Spacing and Troponin-T degradation

There was no treatment effect on sarcomere length ($P>0.05$; table 1 and figure 5). However, there was a tendency for treatment effect on muscle fiber spacing that the 10 kV and control samples tended to have greater muscle fiber spacing compared to those from the 2.5 kV treatments, while the muscle fiber spacing was not different for the 5 kV treatment when compared to those from any of the other treatments ($P=0.09$; table 1 and figure 7). There was no three-way interaction of treatment x aging x display nor interactions of treatment x aging or treatment x display for troponin-T degradation ($P>0.05$; figure 6). In addition, there was no main effect of treatment effect on troponin-T degradation ($P>0.05$; table 1). As expected, there was an aging x display interaction ($P<0.05$; table 2), where samples aged for 14 days and retail displayed 7 days showed the highest relative percentage of degraded troponin-T, and samples aged for 0 days with no retail display showed the lowest relative percentage of degraded troponin-T compared to all other aging and retail display periods ($P<0.05$). Samples aged for 14 days with no retail display showed no difference in troponin-T degradation with those from samples aged 0 days but retail displayed for 7 days ($P<0.05$).

Zhang et al. (2017) and Qi et al. (2012) both found that sarcomere length can be shortened after multiple cycles of freezing and thawing. While the exact nature of how the formation of ice crystals can impact sarcomere length is not yet fully understood, the current hypothesis is that the formation of the ice crystals can cause the sarcomeres to expand. When the

ice crystals melt, the sarcomeres will contract back to their original position (Qi et al., 2012). However, the repeated freeze-thaw cycle can cause extensive damage to the sarcomere and result in eventual collapse of Z-disk leading to sarcomere shortening. Qian et al. (2019) observed that application of 2.5kV EF while thawing beef striploin could prevent this noted shortening of sarcomeres from the repeated freeze-thaw cycle, and thus improve water-holding capacity. There were no differences in sarcomere length among the treatments in our study, which could be explained that our study only had one freezing cycle and that the ice crystals were not allowed to re-form multiple times thus not resulting in collapse of Z-disk.

Due to the characteristic of water as a dipole, it is possible that the ice crystals can break apart when ions move back and forth in the presence of AC in the form of EF (Mukherjee et al., 2021). Therefore, our thought process was that if EF treatments can reduce ice crystal size in the extracellular space, we should observe reduced spacing between muscle fibers. The 10 kV treatment did not reduce the spacing between muscle fibers in our study, but the 2.5 kV treatment has a tendency to have smaller muscle fiber spacing compared to the control. Qian et al. (2019) also observed that when thawing beef striploin under 2.5kV, the EF treatment reduced the distance of the gaps between muscle fibers. Furthermore, Lung et al. (2022) found that Peking duck that was thawed under a pulsed electric field voltages of 1-3kV had lower average distance between the muscle fibers compared to the control. However, it is interesting to note that when the same authors showed that applying pulsed electric field at 4kV failed to decrease distance between muscle fibers which resulted similar gap distance compared to those from the traditionally thawed samples (Lung et al., 2022). Van der Sman (2017) hypothesized that increasing voltage can cause additional damage to the microstructure of meat from the heat generated, resulting in increased distances between muscle fibers. Perhaps, this could be used to

explain why only the 2.5kV treatment had a tendency to reduce muscle fiber spacing compared to the control.

As a result of the ion movement caused by the AC of the EF, we anticipated increased protein denaturation caused by the damage. Mousakhani-Ganjeh et al. (2015) observed that frozen tuna fish thawed under 4.5kV-14kV showed increased protein denaturation as the voltage intensity increased compared to air thawing. Calpain is a major proteolytic enzyme that can be easily denatured like other proteins (Zhang and Ertbjerg, 2018), which Qian et al. (2019) hypothesized that calpain activity can be inhibited by the EF. This is further supported by Ko et al. (2016) who found tilapia stored at refrigeration under an EF of 3kV-9kV delayed enzymatic activity, which included calpains activity. These findings warrant further investigation on the impacts of an EF on the enzymatic activity of calpains and how this can impact the degradation of myofibrillar proteins.

Subjective Color Evaluation

There was a three-way interaction among treatment x aging x display for the objective discoloration evaluated by the trained panelists ($P<0.05$; figure 8). Overall, there was an anticipated impact on discoloration as samples progressed during display ($P<0.05$). For samples aged 0 days, there was no significant difference in discoloration among the treatments till day 6 of retail display. The 5 kV treated samples showed more discoloration on day 6 and 7 of retail display compared to samples from the rest of the treatments ($P<0.05$).

For samples aged for 14 days, the increased aging time resulted in much greater overall discoloration compared to those aged for 0 days ($P<0.05$). There was no significant difference in discoloration among the aged treatments until day 3 of retail display. On day 3, 4 and 5, the 0 kV and 2.5 kV samples were more discolored than the 5 kV and 10 kV samples ($P<0.05$). The

treatments showed the most variability on day 6, with 0 kV samples having more discoloration than 2.5 kV and 10 kV, and 5 kV had the least discoloration compared to all other EF treatments (P<0.05). The 0 kV and 10 kV samples showed more discoloration on day 7 of retail display compared to 2.5 kV and 5 kV samples (P<0.05).

The impact of EF showed varying impacts on color stability during thawing. Ko et al. (2016) assessed the freshness of whole tilapia fish stored at refrigeration temperatures under EF ranging from 3kV-9kV and found that samples treated with 9kV EF took longer to emit a spoiled odor to trained panelists, and all EF treatments improved the brightness of the belly appearance compared to those from the control. Zhang et al. (2023) also found that yellow croaker fish stored partially frozen under a 3kV EF showed increased freshness characteristics when compared to the control. The freshness characteristics included odor, gill color, eyeball appearance, and surface color, which were all evaluated by trained panelists. These studies indicate that application of EF has the potential to preserve the appearance of freshness for various animal proteins.

Objective Color Evaluation

There was no three way interaction of treatment x display x aging, and there was no treatment x display nor treatment x aging interactions for L* values (P>0.05). Finally, there was no main effect of treatment for L* values (P>0.05). There was no three-way interaction of treatment x aging x display for a* values (P>0.05), but there was an interaction of treatment x aging (P<0.05; figure 9). For samples aged 0 days, there was no impact of treatments on a* values (P>0.05). For samples aged 14 days, the 5 kV samples had the higher a* values than all other EF treatments (P<0.05), followed by 2.5 kV and 10 kV samples having lower a* values

than 5 kV (P<0.05), with 0 kV samples having the lowest a* value but no different from 2.5 kV samples (P>0.05).

There was also an interaction of treatment x display for a* values on all days except for day 7 of display (P<0.05; figure 10). When evaluating a* values across display, all treatment samples displayed progressive decline of a* values (P<0.05). On day 0, all EF treatments had higher a* compared to the 2.5 kV samples (P<0.05). On days 1-3, 5 kV samples had greater a* values than those from 2.5 kV (P<0.05), but not different than those from the 0 kV and 10 kV samples (P>0.05). On day 4 and 5, the 5 kV samples had higher a* values than the those from 0 kV and 2.5 kV samples (P<0.05), but were not different to those from the 10 kV samples (P>0.05). On day 6, the 5 kV treated samples had higher a* values than the 10 kV samples, but both the 5 kV and 10 kV samples were not different from the 0 kV and 2.5 kV samples (P<0.05). All treatments reached the same a* value on day 7 (P>0.05).

There was no three-way interaction of treatment x aging x display for b* values nor an interaction of treatment x display (P>0.05). However, there was an interaction for treatment x aging for b* values (P<0.05; figure 11). For samples aged 0 days, there was no impact of treatments on b* values (P>0.05). However, when considering the samples aged 14 days, the 5 kV treatment had the highest b* values compared to those from all other EF treatments (P<0.05).

He et al. (2013) demonstrated that pork loins thawed under a 10 kV EF had greater L* values compared to those from the control samples, but there was no impact on a* and b* values. On the other hand, Jia et al. (2017) showed that all EF treatments increased L*, a*, and b* values of frozen rabbit meat compared to those from conventionally thawed, and as voltages increased from 5-15 kV to 20 kV and 25 kV, the L* and a* values further increased. Qian et al. (2019) further showed that beef striploin treated with 2.5 kV EF improved a* during the first 24 hours of

the thawing process compared to those from traditional thawing. In our study, there was no EF impact on L*, but EF treatments improved a* for the steaks aged 14 days, particularly for the 5 kV treatment. Along with this finding, there was a reduction in discoloration for the 2.5 kV and 5 kV EF treated samples after 14 days of aging. In addition to this, there was an observed decrease in b* values for samples aged for 14 days. When meat is fresher, there are higher level of antioxidants available to maintain the redness of meat longer, which could explain why the a* and b* of 0 days aged samples were unaffected by the EF treatment (Echegaray et al., 2021). Maggiolino et al. (2020) observed that an increase of antioxidants status of beef ribeye could improve b* values as well as a*. Many forms of antioxidants such as proteins, peptides, and vitamins naturally present in muscle cells and function as color stabilizers through protecting the myoglobin from oxidation (Suman and Joseph, 2013). Joseph et al. (2012) observed that increased abundance of these color stabilizing agents was positively correlated to increased redness in beef *Longissimus lumborum*. It is possible that the application of EF can enhance the activity of these antioxidants that presented in the striploins, and thus led to the improvement in a* values and prevent metmyoglobin formation.

Warner-Bratzler Shear Force

There was no three-way interaction of treatment x aging x display nor 2-way interactions of treatment x display or interaction of treatment x aging on WBSF ($P>0.05$). However, there was also a main effect of treatment on WBSF ($P<0.05$; table 1). The 10 kV samples had lower WBSF compared to those from 5 kV and 0 kV samples ($P<0.05$), while WBSF from 2.5 kV samples were not different from those from the 10 kV treated samples ($P>0.05$). There was an expected display x aging interaction ($P<0.05$; table 2). Samples aged for 0 days with no retail display had the highest WBSF compared to all other aging and retail display periods ($P<0.05$).

Samples aged for 14 days had the lowest WBSF compared to samples aged for 0 days regardless of retail display period ($P<0.05$).

Qian et al. (2019) also observed a reduction in slice shear force values for beef striploin thawed under a 2.5 kV EF compared to those from traditional thawing. It was to our surprise that the 10 kV treated samples had a lower shear force than all other treatments in our study. However, this improvement in tenderness in our study did not derive from the calpain system nor muscle contractile status, as there were no differences in troponin-T degradation nor sarcomere length within all EF treatments. Additionally, the 10 kV EF treated samples did not have an increased muscle fiber spacing compared to the control and 5 kV EF treatment. Qian et al. (2019) found that the application of 2.5 kV EF decreased muscle fiber cracking, which is the phenomenon of one muscle fiber splits into two in response to damage, thus requiring more force to shear through the increased number of muscle fibers and decreasing tenderness (Chang et al., 2021). The authors hypothesized such effects may be responsible for the observed increase in tenderness (Qian et al., 2019). Therefore, further investigation looking at the structure of muscle fibers could explain the impacts on tenderness observed in this study.

Lipid Oxidation and Oxygen Radical Absorbance Capacity (ORAC)

There were no interactions of treatment x aging x display, treatment x aging, aging x display, nor treatment x display on lipid oxidation ($P>0.05$). Additionally, there was no main effect of treatment nor aging on lipid oxidation ($P>0.05$; table 1). Finally, there was a main effect of display, where there was an anticipated observed increase in lipid oxidation in samples displayed for 7 days compared to samples subjected to 0 days retail display ($P<0.05$).

For the hydrophilic ORAC, there was no three-way interaction among treatment x aging x display nor any main effect of treatment ($P>0.05$; table 1); however, there was an aging x

display interaction ($P<0.05$; table 2). Samples aged for 14 days followed by 7 days display had the highest, followed by samples aged for 14 days with no retail display and samples with no additional aging time with 7 days of retail display, with samples with no additional aging period or display period having the lowest Trolox equivalent/g of meat compared to those from other aging and display periods ($P<0.05$). For lipophilic ORAC, there was no three-way interaction among treatment x aging x display, no aging x display interaction, nor any treatment effect ($P>0.05$; table 1); however, there was a main effect of aging *(*$P<0.05$). Samples that were aged for 14 days had higher Trolox equivalent/g of meat compared to samples with no additional aging period ($P<0.05$).

When looking at the effect of EF on lipid oxidation of meat in other research, Jia et al. (2017) observed that all rabbit meat samples treated with EF, regardless of voltage intensity, showed decreased lipid oxidation values compared to those thawed without EF. However, Mousakhani-Ganjeh et al. (2016a) showed that increasing voltage showed increased lipid oxidation in frozen tuna fish during thawing. In our study, we did not observe the application of EF having an impact on lipid oxidation of the samples. However, it was to our surprise that we did not find an aging effect for lipid oxidation in this study as lipid oxidation typically increases with increased aging time (Brewer and Wu, 1993; Koutsidis et al., 2008).

In agreement with the lipid oxidation finding, we also found that EF did not enhance antioxidant capacity regardless of voltages applied. This finding aligns with Sánchez-Moreno et al. (2005) who found that application of an EF did not alter 2,2-diphenyl-1picrylhydrazl (DPPH) radical scavenging capacity in orange juice. However, with this finding, our hypothesis that antioxidant activity was increased by the EF and resulted in improvements in color stability was proven incorrect. On the other hand, our results did show that antioxidant capacity increased with

aging time for both the lipophilic and hydrophilic portions. The ORAC method relies upon adding a free radical to the system of a sample and seeing how the antioxidants present protect the fluorescent output (Huang et al., 2002). The principle indicates that the longer there is fluorescence in the system, the higher the activity of the antioxidants present. A limitation with this is as an estimation of the activity and not necessarily the amount of antioxidants that are present in the sample, as there can be non-specific binding as well as issues with the photostability of the fluorescence. There are other assays that could be done in conjunction with ORAC to provide insight into the antioxidant profile such as the hydroxyl radical averting assay, an ET-based method, and total phenol content through a Folin-Ciocalteu assay (Echegaray et al., 2021). Therefore Liu et al. (2017) also observed that as aging progressed, the antioxidant capacity gradually increased in duck meat. Neri et al. (2020) found when freezing plant foods that the damage of cellular breakages can cause a release of antioxidant compounds out of being confined into the cells. Perhaps, the cellular damage that occurred during freezing caused antioxidant enzymes and peptides bound in the muscle fibers be released into the extracellular space over the 14 days aging time, which mitigated the generation of secondary lipid oxidation products during aging time.

Conclusions

The results from this research provided valuable insight into the function of the EF and its capabilities to potentially improve frozen beef quality. Although our results showed the application of EF to beef did not improve yield or thawing time as originally expected, there were indications that this technology may improve post-thawing quality such as tenderness and shelf-stability of beef. Further investigation should look deeper into how different voltages can impact structural damage to the muscle during thawing and how the damage relates to tenderness

as well as impacts on enzymatic activity. Finally, other research has shown that intervening with EF prior to the freezing step may be a more efficient way to improve yield and thawing losses of previously frozen meat products compared to intervening after freezing as occurred.

References

AMSA. 2016. Research guidelines for cookery, sensory evaluation, and instrumental tenderness measurements of meat. *Am. Meat Sci.* Assoc. Champaign, IL.

AOAC International. (2000a). AOAC Official Method 950.46 *Moisture in Meat.* 17th ed. AOAC, Arlington, VA.

AOAC International. (2000b). AOAC Official Method 992.15 *Crude Protein in Meat and Meat Products Including Pet Food*. 17th ed. AOAC, Arlington, VA.

Balan, P., Y. H. B. Kim, A. D. Stuart, R. Kemp, M. Staincliffe, C. Craigie, and M. M. Farouk. 2019. Effect of fast freezing then thaw-aging on meat quality attributes of lamb M. longissimus lumborum. *Anim. Sci. J.* 90(8):1060-1069. https://doi.org/10.1111/asj.13216

Brewer, M., and S. Wu. 1993. Display, packaging, and meat block location effects on color and lipid oxidation of frozen lean ground beef. *J. Food Sci.* 58(6):1219-1236. https://doi.org/10.1111/j.1365-2621.1993.tb06152.x

Chun, C. K., M. Roth, R. Welti, M. P. Richards, W.-W. Hsu, T. O'Quinn, and M. D. Chao. 2023. Exploring the potential effect of phospholipase A2 antibody to extend beef shelf-life in a beef liposome model system. *Meat Sci.* 198:109091. https://doi.org/10.1016/j.meatsci.2022.109091

Costa, R. M., F. A. Oliveira, O. Delaney, and V. Gekas. 1999. Analysis of the heat transfer coefficient during potato frying. *J. Food Eng.* 39(3):293-299. https://doi.org/10.1016/S0260-8774(98)00169-1

Dahmer, P. L., F. B. McDonald, C. K. Chun, C. A. Zumbaugh, C. K. Jones, A. R. Crane, T. Kott, J. M. Lattimer, and M. D. Chao. 2022. Evaluating the impact of feeding dried distillers

grains with solubles on Boer goat growth performance, meat color stability, and antioxidant capacity. *Transl. Anim. Sci.* 6(2):txac060. https://doi.org/10.1093/tas/txac060

Echegaray, N., M. Pateiro, P. E. Munekata, J. M. Lorenzo, Z. Chabani, M. A. Farag, and R. Domínguez. 2021. Measurement of antioxidant capacity of meat and meat products: methods and applications. *Molecules*. 26(13):3880. https://doi.org/10.3390%2Fmolecules26133880

Fagan, J. A., P. J. Sides, and D. C. Prieve. 2005. Evidence of multiple electrohydrodynamic forces acting on a colloidal particle near an electrode due to an alternating current electric field. *Langmuir*. 21(5):1784-1794. https://doi.org/10.1021/la048076m.

Grunert, K. G., L. Bredahl, and K. Brunsø. 2004. Consumer perception of meat quality and implications for product development in the meat sector—a review. *Meat Sci*. 66(2):259-272. https://doi.org/10.1016/S0309-1740(03)00130-X.

Hammond, P. A., C. K. Chun, W. J. Wu, A. A. Welter, T. G. O'Quinn, G. Magnin-Bissel, E. R. Geisbrecht, M. D. Chao, and T. G. O'Quinn. 2022. An investigation on the influence of various biochemical tenderness factors on eight different bovine muscles. *Meat Muscle Biol.* 6(1):1-17. https://doi.org/10.22175/mmb.13902

He, X., R. Liu, S. Nirasawa, D. Zheng, and H. Liu. 2013. Effect of high voltage electrostatic field treatment on thawing characteristics and post-thawing quality of frozen pork tenderloin meat. *J. Food Eng.* 115(2):245-250. http://dx.doi.org/10.1016/j.jfoodeng.2012.10.023

Heinz, G., and P. Hautzinger. 2007. Meat processing technology for small to medium scale producers. Food and Agricultural Organization of the United Nations. 7(11):470. ISBN: 978-974-7946-99-4. https://www.fao.org/documents/card/fr/c/fb92d00f-7ff3-593a-a77c-.

Hsieh, C. W., C. H. Lai, W. J. Ho, S. C. Huang, and W. C. Ko. 2010. Effect of thawing and cold storage on frozen chicken thigh meat quality by high-voltage electrostatic field. *J. Food Sci.* 75(4):193-197. http://dx.doi.org/10.1111/j.1750-3841.2010.01594.x.

Huang, D., B. Ou, M. Hampsch-Woodill, J. A. Flanagan, and R. L. Prior. 2002. High-throughput assay of oxygen radical absorbance capacity (ORAC) using a multichannel liquid handling system coupled with a microplate fluorescence reader in 96-well format. *J. Agr. Food Chem*. 50(16):4437-4444. https://doi.org/10.1021/jf0201529.

Jia, G., H. Liu, S. Nirasawa, and H. Liu. 2017. Effects of high-voltage electrostatic field treatment on the thawing rate and post-thawing quality of frozen rabbit meat. *Innov. Food Sci. Emerg.* 41:348-356. http://dx.doi.org/10.1016/j.ifset.2017.04.011.

Jia, G., S. Nirasawa, X. Ji, Y. Luo, and H. Liu. 2018. Physicochemical changes in myofibrillar proteins extracted from pork tenderloin thawed by a high-voltage electrostatic field. *Food Chem.* 240:910-916. https://doi.org/10.1016/j.foodchem.2017.07.138.

Joseph, P., S. P. Suman, G. Rentfrow, S. Li, and C. M. Beach. 2012. Proteomics of muscle-specific beef color stability. *J. Agr. Food Chem.* 60(12):3196-3203. https://doi.org/10.1021/jf204188v.

Kim, Y. H. B., C. Liesse, R. Kemp, and P. Balan. 2015. Evaluation of combined effects of ageing period and freezing rate on quality attributes of beef loins. *Meat Sci.* 110:40-45. https://doi.org/10.1016/j.meatsci.2015.06.015.

King, D. A., M. C. Hunt, S. Barbut, J. R. Claus, D. P. Cornforth, P. Joseph, Y. H. B. Kim, G. Lindahl, R. A. Mancini, and M. N. Nair. 2023. American meat science association guidelines for meat color measurement. *Meat Muscle Biol.* 6(4):1-81. https://doi.org/10.22175/mmb.12473.

Ko, W.-C., H.-Z. Shi, C.-K. Chang, Y.-H. Huang, Y.-A. Chen, and C.-W. Hsieh. 2016. Effect of adjustable parallel high voltage on biochemical indicators and actomyosin Ca2+-ATPase from tilapia (Orechromis niloticus). *LWT Food Sci. Technol.* 69:417-423. http://dx.doi.org/10.1016/j.lwt.2016.01.074.

Koutsidis, G., J. Elmore, M. J. Oruna-Concha, M. M. Campo, J. D. Wood, and D. Mottram. 2008. Water-soluble precursors of beef flavour. Part II: Effect of post-mortem conditioning. *Meat Sci.* 79(2):270-277. https://doi.org/10.1016/j.meatsci.2007.09.010.

Kropf, D., and H. Zerby. 2002. Meat display lighting. *FACTS National Pork Board*. 4623:1-8. https://porkgateway.org/resource/meat-display-lighting/.

Leygonie, C., T. J. Britz, and L. C. Hoffman. 2012. Impact of freezing and thawing on the quality of meat. *Meat Sci.* 91(2):93-98. https://doi.org/10.1016/j.meatsci.2012.01.013.

Li, D., S. Jia, L. Zhang, Q. Li, J. Pan, B. Zhu, W. Prinyawiwatkul, and Y. Luo. 2017. Post-thawing quality changes of common carp (Cyprinus carpio) cubes treated by high voltage electrostatic field (HVEF) during chilled storage. *Innov. Food Sci. Emerg.* 42:25-32. http://dx.doi.org/10.1016/j.ifset.2017.06.005.

Liu, D., X. Chen, J. Huang, M. Huang, and G. Zhou. 2017. Generation of bioactive peptides from duck meat during post-mortem aging. *Food Chem.* 237:408-415. https://doi.org/10.1016/j.foodchem.2017.05.094.

Lu, N., J. Ma, and D.-W. Sun. 2022. Enhancing physical and chemical quality attributes of frozen meat and meat products: Mechanisms, techniques and applications. *Trends Food Sci. Techn.* 124:63-85. https://doi.org/10.1016/j.tifs.2022.04.004.

Lung, C.-T., C.-K. Chang, F.-C. Cheng, C.-Y. Hou, M.-H. Chen, S. P. Santoso, B. Yudhistira, and C.-W. Hsieh. 2022. Effects of pulsed electric field-assisted thawing on the

characteristics and quality of Pekin duck meat. *Food Chem.* 390:133-137. https://doi.org/10.1016/j.foodchem.2022.133137.

Maggiolino, A., J. M. Lorenzo, A. Salzano, M. Faccia, F. Blando, M. P. Serrano, M. Latorre, J. Quiñones, and P. De Palo. 2020. Effects of aging and dietary supplementation with polyphenols from Pinus taeda hydrolysed lignin on quality parameters, fatty acid profile and oxidative stability of beef. *Anim. Prod. Sci.* 60(5):713-724. http://dx.doi.org/10.1071/AN19215.

Marsh, B., and J. Thompson. 1958. Rigor mortis and thaw rigor in lamb. *J. Sci. of Food Agr.* 9(7):417-424. https://doi.org/10.1002/jsfa.2740090707

Mousakhani-Ganjeh, A., N. Hamdami, and N. Soltanizadeh. 2015. Impact of high voltage electric field thawing on the quality of frozen tuna fish (Thunnus albacares). *J. Food Eng.* 156:39-44. https://doi.org/10.1016/j.jfoodeng.2015.02.004.

Mousakhani-Ganjeh, A., N. Hamdami, and N. Soltanizadeh. 2016a. Effect of high voltage electrostatic field thawing on the lipid oxidation of frozen tuna fish (Thunnus albacares). *Innov. Food Sci. Emerg.* 36:42-47. http://dx.doi.org/10.1016%2Fj.ifset.2016.05.017.

Mousakhani-Ganjeh, A., N. Hamdami, and N. Soltanizadeh. 2016b. Thawing of frozen tuna fish (Thunnus albacares) using still air method combined with a high voltage electrostatic field. *J. Food Eng.* 169:149-154. http://dx.doi.org/10.1016/j.jfoodeng.2015.08.036.

Mukherjee, R., S. F. Ahmadi, H. Zhang, R. Qiao, and J. B. Boreyko. 2021. Electrostatic jumping of frost. *ACS Nano.* 15(3):4669-4677. https://doi.org/10.1021/acsnano.0c09153.

Neri, L., M. Faieta, C. Di Mattia, G. Sacchetti, D. Mastrocola, and P. Pittia. 2020. Antioxidant activity in frozen plant foods: Effect of cryoprotectants, freezing process and frozen storage. *Foods*. 9(12):1886. https://doi.org/10.3390/foods9121886.

Qi, J., C. Li, Y. Chen, F. Gao, X. Xu, and G. Zhou. 2012. Changes in meat quality of ovine longissimus dorsi muscle in response to repeated freeze and thaw. *Meat Sci.* 92(4):619-626. https://doi.org/10.1016/j.meatsci.2012.06.009.

Qian, S., X. Li, H. Wang, W. Mehmood, M. Zhong, C. Zhang, and C. Blecker. 2019. Effects of low voltage electrostatic field thawing on the changes in physicochemical properties of myofibrillar proteins of bovine Longissimus dorsi muscle. *J. Food Eng.* 261:140-149. https://doi.org/10.1016/j.jfoodeng.2019.06.013.

Rahbari, M., N. Hamdami, H. Mirzaei, S. M. Jafari, M. Kashaninejad, and M. Khomeiri. 2018. Effects of high voltage electric field thawing on the characteristics of chicken breast protein. *J. Food Eng.* 216:98-106. http://dx.doi.org/10.1016/j.jfoodeng.2017.08.006.

Sale, A., and W. Hamilton. 1967. Effects of high electric fields on microorganisms: I. Killing of bacteria and yeasts. *BBA Gen. Subjects.* 148(3):781-788. https://doi.org/10.1016/0304-4165(67)90052-9.

Sánchez-Moreno, C., L. Plaza, P. Elez-Martínez, B. De Ancos, O. Martín-Belloso, and M. P. Cano. 2005. Impact of high pressure and pulsed electric fields on bioactive compounds and antioxidant activity of orange juice in comparison with traditional thermal processing. *J. Agr. Food Chem.* 53(11):4403-4409. https://doi.org/10.1021/jf048839b.

Suman, S. P., and P. Joseph. 2013. Myoglobin chemistry and meat color. *Annu. Rev. Food Sci. Technol.* 4:79-99. https://doi.org/10.1146/annurev-food-030212-182623.

Traore, S., L. Aubry, P. Gatellier, W. Przybylski, D. Jaworska, K. Kajak-Siemaszko, and V. Santé-Lhoutellier. 2012. Higher drip loss is associated with protein oxidation. *Meat Sci.* 90(4):917-924. https://doi.org/10.1016/j.meatsci.2011.11.033.

Unal, R., A. E. Yousef, and C. P. Dunne. 2002. Spectrofluorimetric assessment of bacterial cell membrane damage by pulsed electric field. *Innov. Food Sci. Emerg.* 3(3):247-254. https://doi.org/10.1016/S1466-8564(02)00033-4.

Van der Sman, R. 2017. Model for electrical conductivity of muscle meat during Ohmic heating. *J. Food Eng.* 208:37-47. https://doi.org/10.1016/j.jfoodeng.2017.03.029.

Watanabe, G., M. Motoyama, I. Nakajima, and K. Sasaki. 2018. Relationship between water-holding capacity and intramuscular fat content in Japanese commercial pork loin. *Asian Austral J. Anim. Sci.* 31(6):914. https://doi.org/10.5713%2Fajas.17.0640.

Wei, S., X. Xiaobin, Z. Hong, and X. Chuanxiang. 2008. Effects of dipole polarization of water molecules on ice formation under an electrostatic field. *Cryobiology.* 56(1):93-99. https://doi.org/10.1016/j.cryobiol.2007.10.173.

Wu, G., C. Yang, H. L. Bruce, B. C. Roy, X. Li, and C. Zhang. 2023. Effects of alternating electric field assisted freezing-thawing-aging sequence on longissimus dorsi muscle microstructure and protein characteristics. *Food Chem.* 409:135266. https://doi.org/10.1016/j.foodchem.2022.135266

Wu, S., X. Xu, N. Yang, Y. Jin, Z. Jin, and Z. Xie. 2022. Inactivation of Escherichia coli O157: H7 in apple juice via induced electric field (IEF) and its bactericidal mechanism. *Food Microbiol.* 102:103928. https://doi.org/10.1016/j.fm.2021.103928.

Xanthakis, E., M. Havet, S. Chevallier, J. Abadie, and A. Le-Bail. 2013. Effect of static electric field on ice crystal size reduction during freezing of pork meat. *Innov. Food Sci. & Emerg.* 20:115-120. https://doi.org/10.1016/j.ifset.2013.06.011.

Zhang, J., L. Fei, P. Cui, N. Walayat, S. Ji, Y. Chen, F. Lyu, and Y. Ding. 2023. Effect of low voltage electrostatic field combined with partial freezing on the quality and microbial

community of large yellow croaker. *Food Res. Int.* 169:112933. https://doi.org/10.1016/j.foodres.2023.112933.

Zhang, M., F. Li, X. Diao, B. Kong, and X. Xia. 2017. Moisture migration, microstructure damage and protein structure changes in porcine longissimus muscle as influenced by multiple freeze-thaw cycles. *Meat Sci.* 133:10-18. https://doi.org/10.1016/j.meatsci.2017.05.019.

Zhang, Y., and P. Ertbjerg. 2018. Effects of frozen-then-chilled storage on proteolytic enzyme activity and water-holding capacity of pork loin. *Meat Sci.* 145:375-382. https://doi.org/10.1016/j.meatsci.2018.07.017.

Figure 1. A representative image of the experiment setup using the electrostatic thawing system which consists of the electrostatic field (EF) generator (red arrow) and a stainless steel meat cart (black arrow).

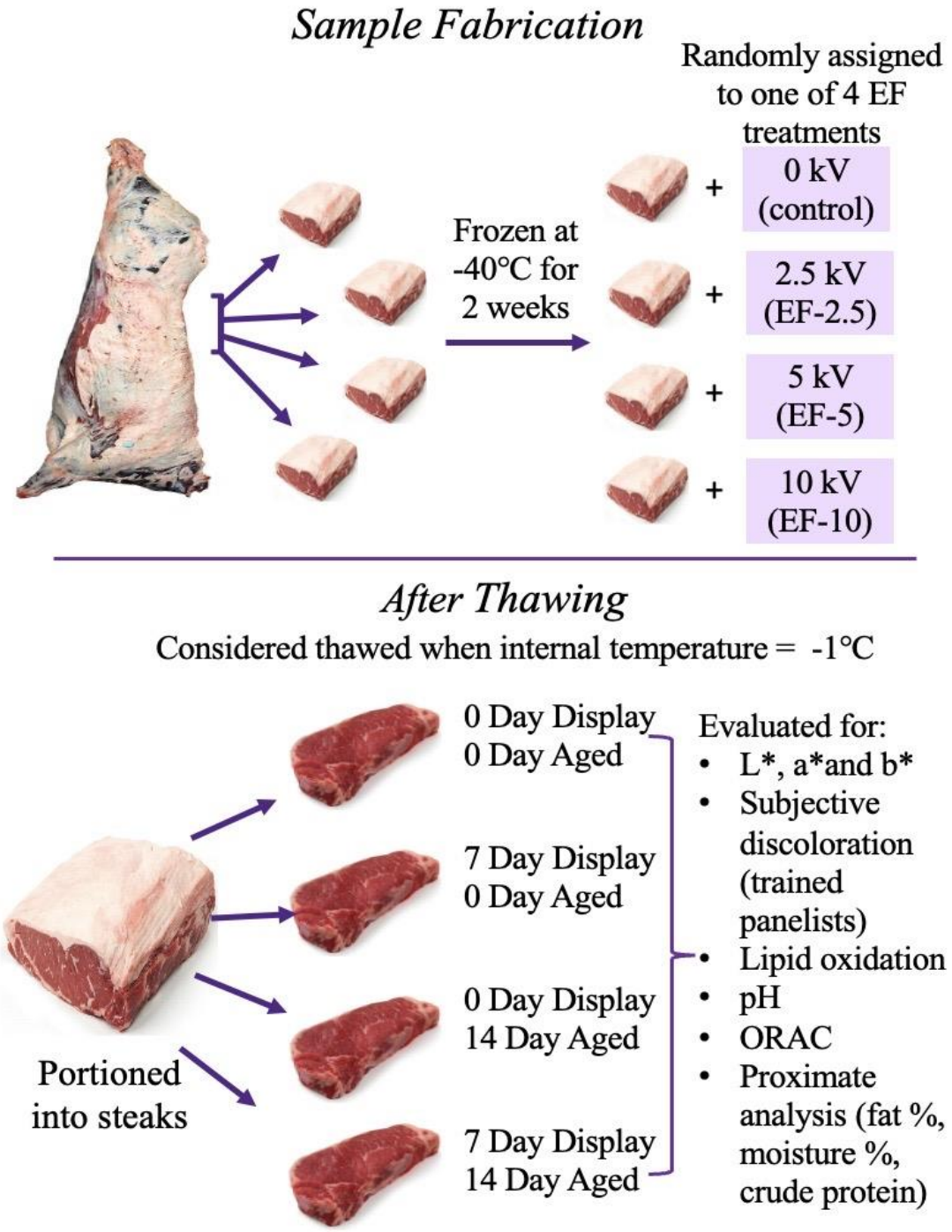

Figure 2. Schematic diagram depicting the experimental design of sample fabrication, treatments, and analysis for each striploin.

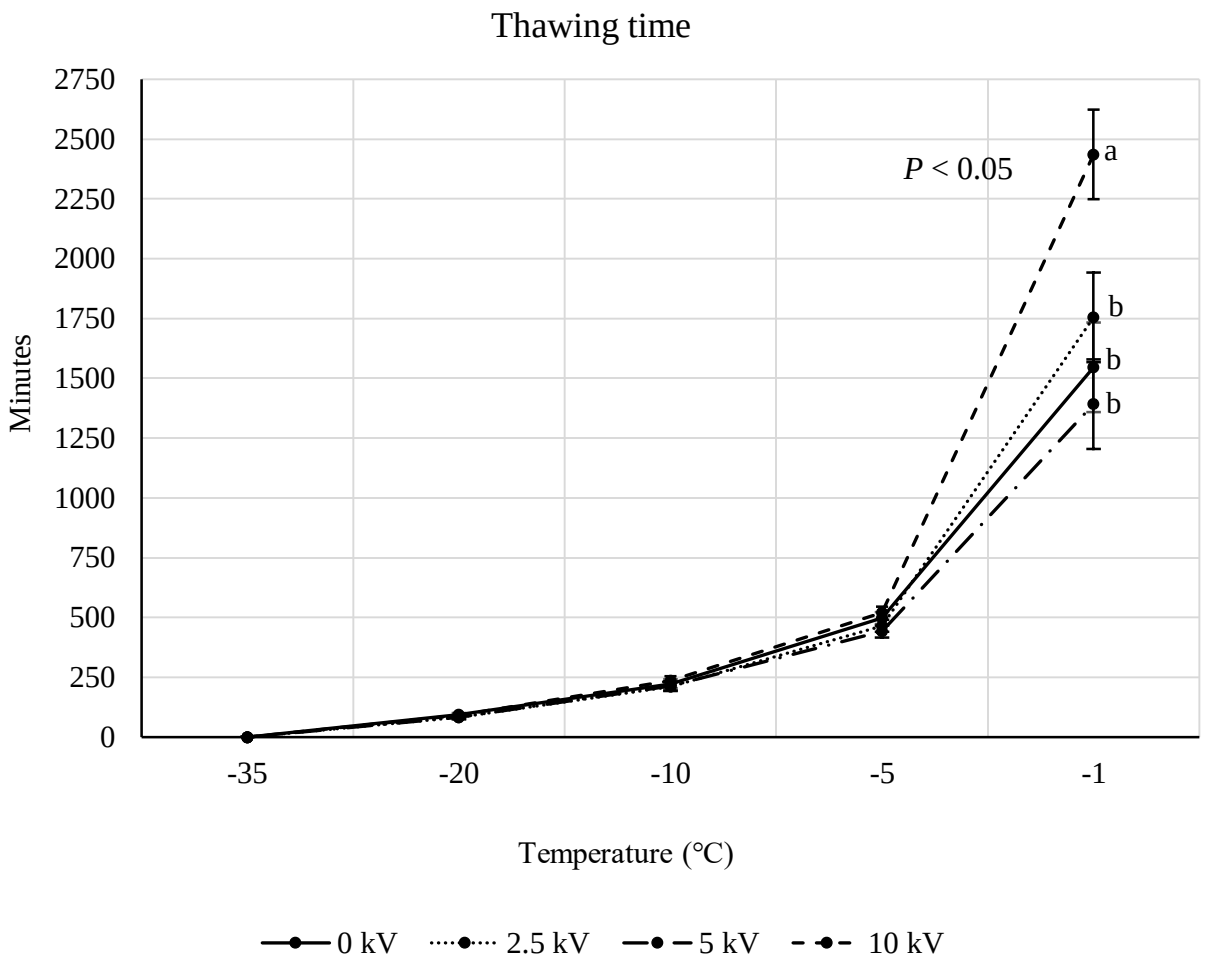

Figure 3. Time (minutes) it takes for striploin halves from each of EF treatments to reach -20, -10, -5 and -1ºC; [a-b] Least square means within a temperature without common superscript differ $P<0.05$.

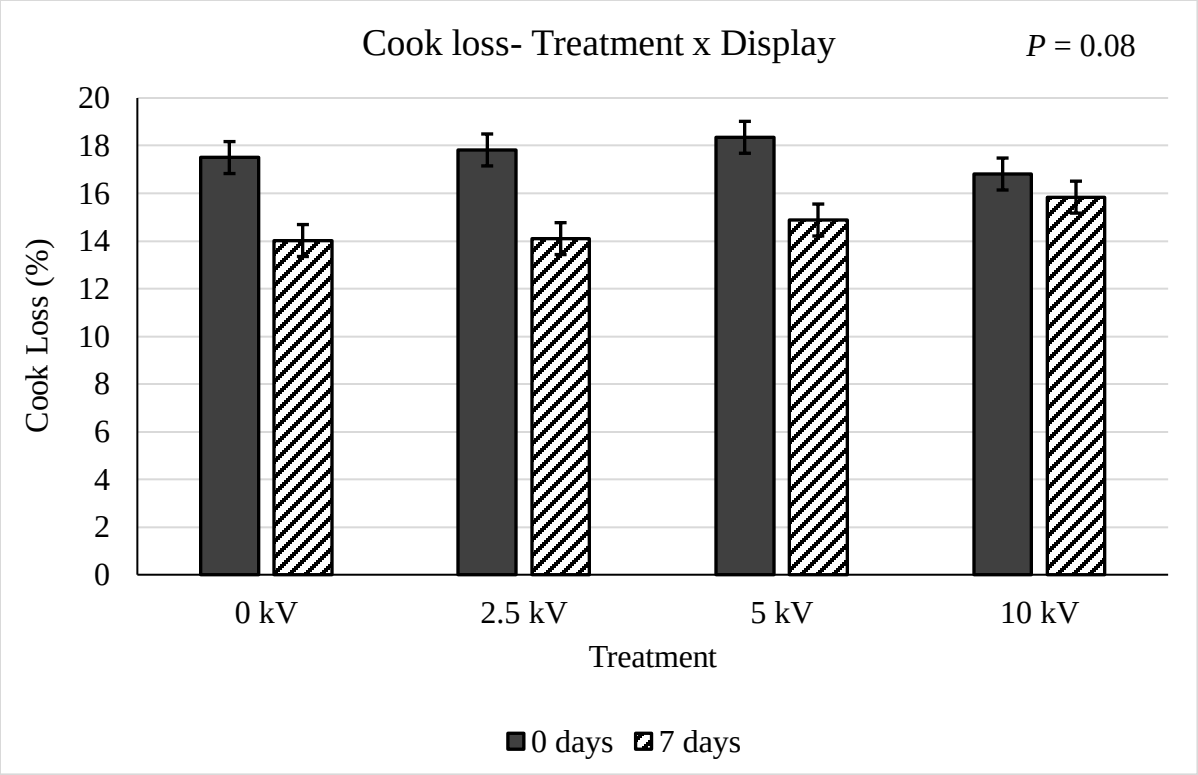

Figure 4. A tendency of treatment and display interaction (P = 0.08) for cooking loss measurement from different EF treatments.

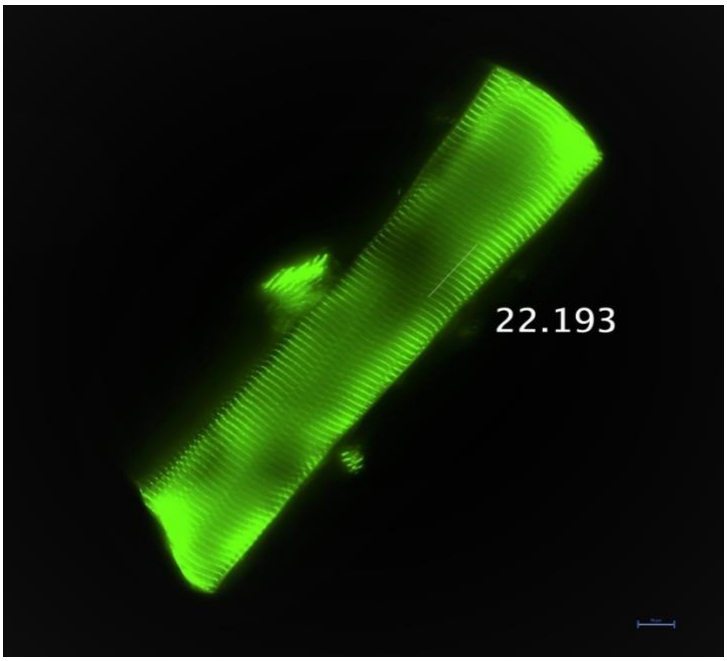

Figure 5. Representative image of sarcomere length measurement featuring 10 sarcomeres being measured (22.19 µm).

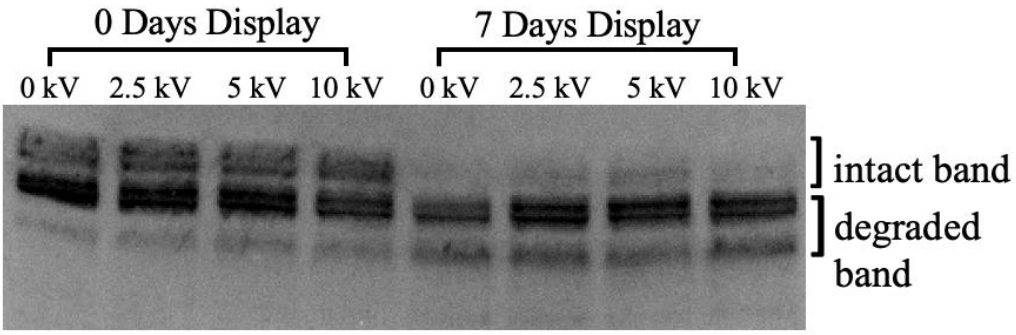

Figure 6. Representative image of troponin-T degradation featuring different display periods demonstrating intact and degraded troponin-T bands.

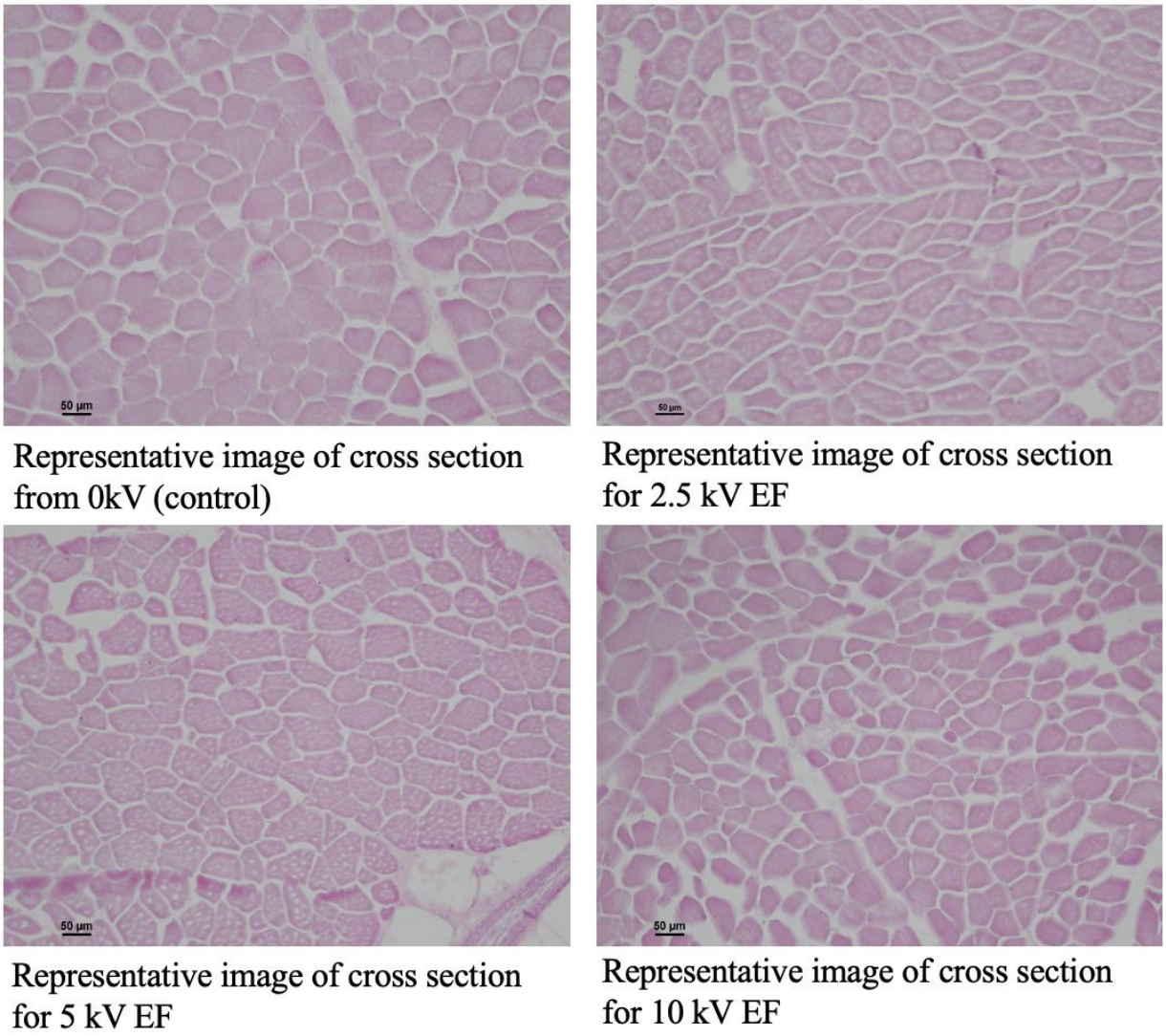

Figure 7. Representative image of muscle fiber cross sections used for muscle fiber spacing measurements for each EF treatment (muscle fiber - red and extracellular space - white).

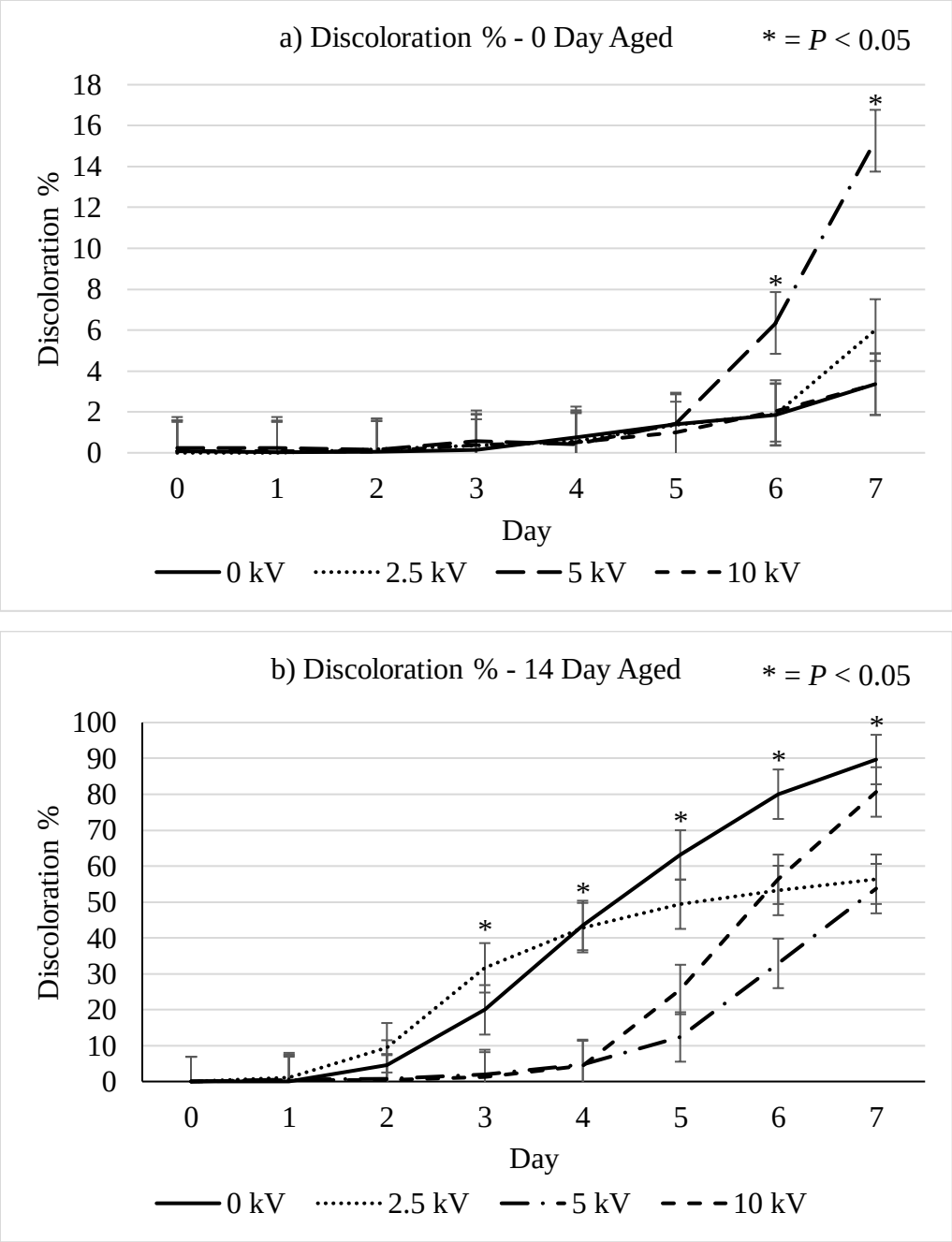

Figure 8. Discoloration % of samples from the EF thawing treatments during 7 days of retail display for a) unaged samples and b) aged for 14 days after thawing. The * indicated days there were significant differences in discoloration % ($P < 0.05$).

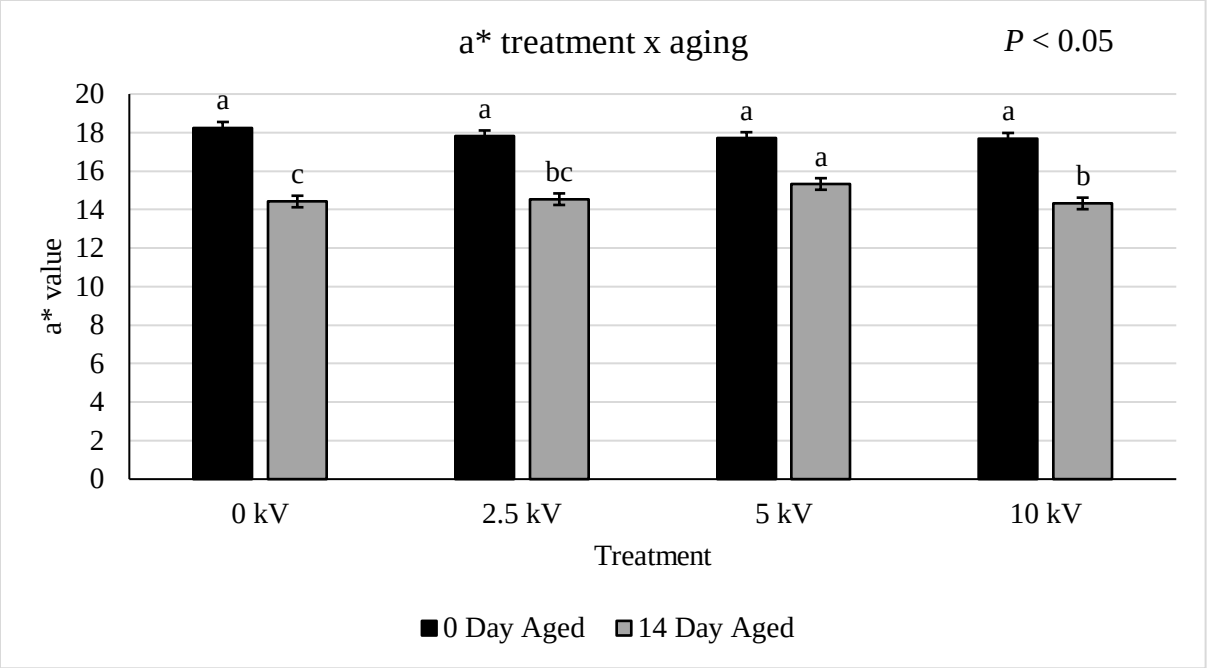

Figure 9. a* values of samples from the EF thawing treatments for unaged and aged for 14 days after thawing; [a-c] = $P<0.05$ within each aging period.

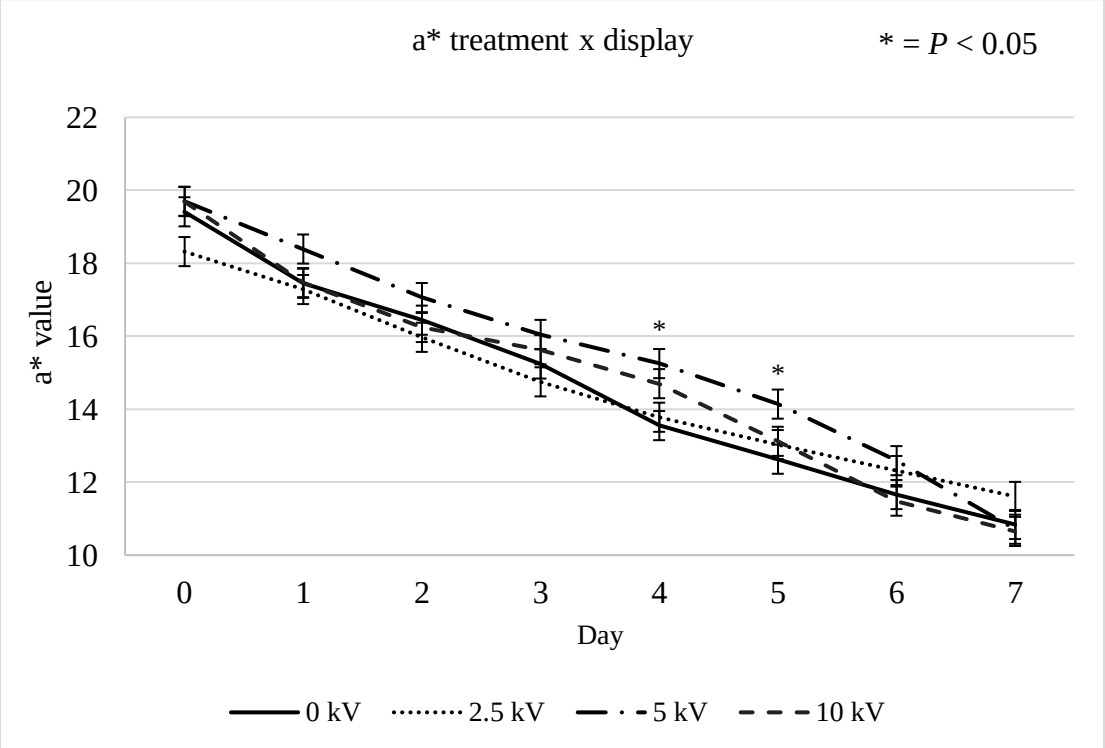

Figure 10. Interaction of treatment x display for a* values of samples from the EF thawing treatments during 7 days of retail display. The * indicated days there were significant differences in a* ($P < 0.05$).

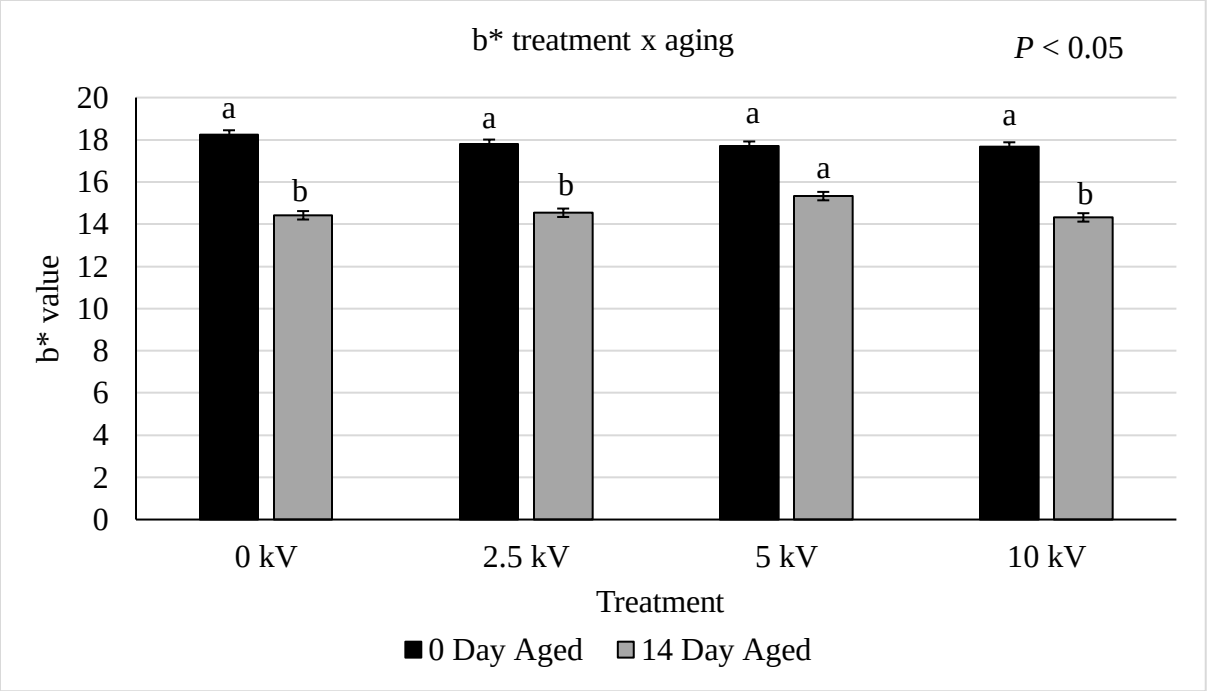

Figure 11. Interaction of treatment x aging for b* values of samples from EF thawing treatments for unaged and aged for 14 days after thawing; $^{a-b}$ = P<0.05 within each aging period.

Table 1. Main effect of treatment for purge loss, cook loss, aerobic plate counts, proximate analysis, pH, sarcomere length, muscle fiber spacing, troponin-T degradation, Warner-Bratzler shear force (WBSF), lipid oxidation and oxygen radical absorbance capacity (ORAC) of beef striploins thawed under different EF treatments

	Treatments					
Measurements	0 kV	2.5 kV	5 kV	10 kV	*SEM*[4]	P-value
Purge Loss (%)	1.36[b]	1.72[ab]	1.94[a]	2.20[a]	0.22	< 0.05
Cook Loss (%)	15.76	15.91	16.62	16.33	0.50	0.51
APC-Swab (log CFU/mL)	2.32	2.30	2.20	2.42	0.08	0.22
APC-Purge (log CFU/mL)	2.19	2.11	1.96	2.11	0.08	0.32
Moisture %	70.37	70.46	70.64	70.16	0.43	0.74
Protein %	22.30	22.26	22.42	22.11	0.18	0.45
Fat %	6.50	6.53	6.35	6.84	0.49	0.80
pH	5.67	5.64	5.65	5.65	0.02	0.34
Purge Protein Concentration (mg/mL)	52.49	51.20	49.82	47.20	2.24	0.37
Sarcomere Length (µm)	2.01	1.92	1.89	1.96	0.05	0.17
Muscle Fiber Spacing (µm)	11.25	9.53	10.17	11.47	0.84	0.09
Troponin-T Degradation[1] (%)	88.91	90.00	88.32	89.92	2.03	0.54
WBSF (kgf)	3.33[ab]	3.21[bc]	3.39[a]	3.13[c]	0.15	< 0.05
Lipid Oxidation (mg of MDA[2]/kg of meat)	0.28	0.26	0.26	0.26	0.05	0.98
Hydrophilic ORAC (TE[3]/g of meat)	17.06	16.30	16.23	17.18	0.63	0.33
Lipophilic ORAC (TE/g of meat)	0.33	0.31	0.30	0.31	0.02	0.75

[a-c] Least square means within a row without common superscript differ $P<0.05$

[1] Relative percentage of degraded troponin-T

[2] MDA = Malondialdehyde

[3] TE = Trolox equivalent

[4] Standard error of least square means

Table 2. Effect of aging x display interaction for Warner-Bratzler shear force (WBSF), troponin-T degradation, and hydrophilic oxygen radical absorbance capacity (ORAC) assay of beef striploins thawed under different EF treatments

Aging	Display	WBSF (kgf)	Troponin-T Degradation[1] (%)	Hydrophilic ORAC (TE[2] equivalent/g of meat)
0 Days Aging	0 Days	3.86[a]	77.10[c]	14.24[c]
	7 Days	3.22[b]	91.49[b]	15.76[b]
14 Days Aging	0 Days	3.00[c]	92.24[b]	15.72[b]
	7 Days	2.97[c]	96.33[a]	21.06[a]
	SEM[3]	0.15	1.36	0.65
	P-Value	< 0.05	< 0.05	< 0.05

[a-c] Least square means within a row without common superscript differ $P<0.05$

[1] Relative percentage of degraded troponin-T

[2] TE = Trolox equivalent

[3] Standard error of least square means